

Spectral Analyses Reveal the Presence of Adult-Like Activity in the Embryonic Stomatogastric Motor Patterns of the Lobster, *Homarus americanus*

Kristina J. Rehm, Adam L. Taylor, Stefan R. Pulver, and Eve Marder

Volen Center, Brandeis University, Waltham, Massachusetts

Submitted 11 January 2008; accepted in final form 25 March 2008

Rehm KJ, Taylor AL, Pulver SR, Marder E. Spectral analyses reveal the presence of adult-like activity in the embryonic stomatogastric motor patterns of the lobster, *Homarus americanus*. *J Neurophysiol* 99: 3104–3122, 2008. First published March 26, 2008; doi:10.1152/jn.00042.2008. The stomatogastric nervous system (STNS) of the embryonic lobster is rhythmically active prior to hatching, before the network is needed for feeding. In the adult lobster, two rhythms are typically observed: the slow gastric mill rhythm and the more rapid pyloric rhythm. In the embryo, rhythmic activity in both embryonic gastric mill and pyloric neurons occurs at a similar frequency, which is slightly slower than the adult pyloric frequency. However, embryonic motor patterns are highly irregular, making traditional burst quantification difficult. Consequently, we used spectral analysis to analyze long stretches of simultaneous recordings from muscles innervated by gastric and pyloric neurons in the embryo. This analysis revealed that embryonic gastric mill neurons intermittently produced pauses and periods of slower activity not seen in the recordings of the output from embryonic pyloric neurons. The slow activity in the embryonic gastric mill neurons increased in response to the exogenous application of *Cancer borealis* tachykinin-related peptide 1a (CabTRP), a modulatory peptide that appears in the inputs to the stomatogastric ganglion (STG) late in larval development. These results suggest that the STG network can express adult-like rhythmic behavior before fully differentiated adult motor patterns are observed, and that the maturation of the neuromodulatory inputs is likely to play a role in the eventual establishment of the adult motor patterns.

INTRODUCTION

Many neuronal networks, including those in the spinal cord, retina, and visual system, are spontaneously active before they are required for their adult functions (Moody and Bosma 2005). A large number of studies have focused on when and how this spontaneous network activity is generated and possible roles this activity plays in the proper development of the network (Ben-Ari 2001; Cang et al. 2005; Demas et al. 2006; Fischer et al. 1998; Garaschuk et al. 1998; Greer et al. 2006; Gu and Spitzer 1995; Hanson and Landmesser 2003, 2004, 2006; Hooks and Chen 2006; Huberman et al. 2006; Leinekugel et al. 2002; Mehta and Sernagor 2006; Milner and Landmesser 1999; Moody and Bosma 2005; O'Donovan 1999; Penn et al. 1998; Ren and Greer 2003; Sernagor et al. 2001; Stellwagen and Shatz 2002; Torborg and Feller 2005; Warland et al. 2006).

Studies in the mammalian retina (Demas et al. 2003; Warland et al. 2006; Wong and Oakley 1996; Wong et al. 1993),

spinal cord (Bekoff 1976; Nishimaru and Kudo 2000; Ren and Greer 2003; Sharp et al. 1999), and brain stem (Greer et al. 2006; Pagliardini et al. 2003) have documented the age-related progression of changes from early spontaneous activity to adult-like activity. There are common trends in the maturation of activity patterns: embryonic spontaneous network activity is often episodic and characterized by synchronous firing of many neurons, and this synchronous activity can begin to disappear before eye opening, walking, or breathing. There does not seem to be a universal program, however, for the transition from early spontaneous network activity to mature activity. Spontaneous activity diminishes at different rates along the rat spinal cord (Ren and Greer 2003), whereas in the mouse spinal cord, spontaneous activity disappears at similar times along the spinal cord, but more mature motor patterns appear at different rates along the spinal cord (Yvert et al. 2004). There are also many kinds of transitional activity in different networks. In the mouse retina (Demas et al. 2003), transitional activity is distinct from both the immature and mature activity patterns, but in the spinal cord of the metamorphosing frog, the transitional state includes both immature and mature forms of activity (Combes et al. 2004).

In developing motor systems, one can ask a number of questions. Do mature rhythms appear suddenly or gradually? Do mature and immature motor patterns occur simultaneously in the same neuron? Is there a reliable temporal structure to this transition? Do mature patterns appear in an organized pattern over time, or do they emerge in a more stochastic manner? What is changing in the network and/or inputs to the network that could explain the appearance of mature activity patterns?

The decapod crustacean stomatogastric nervous system (STNS) is a useful system for the study of network maturation because the rhythmic movements of the adult stomach are stereotyped and the neuronal network that controls these motor patterns is relatively small—~30 neurons are contained within the stomatogastric ganglion (STG)—and has been well characterized (Harris-Warrick et al. 1992). The STNS controls a number of rhythmic movements of the stomach. One of these rhythms, the gastric mill rhythm, controls the movements of a set of teeth within the foregut that chews food in the stomach. The adult gastric mill rhythm typically has a frequency of ~0.1 Hz. Another rhythm, the pyloric rhythm, controls the movements of the pylorus, which filters food particles of different sizes. The frequency of the adult pyloric rhythm is typically ~1 Hz. Despite the difference in

Address for reprint requests and other correspondence: E. Marder, Volen Ctr. MS 013, Brandeis Univ., 415 South St., Waltham, MA 02454-9110 (E-mail: marder@brandeis.edu).

The costs of publication of this article were defrayed in part by the payment of page charges. The article must therefore be hereby marked "advertisement" in accordance with 18 U.S.C. Section 1734 solely to indicate this fact.

frequency, these two rhythms are not completely independent. For example, adult motor neurons produce activity reflecting both rhythms at the same time (Bucher et al. 2006; Heinzel 1988; Heinzel and Selverston 1988; Mulloney 1977; Thuma and Hooper 2002; Weimann et al. 1991).

Before hatching, and therefore before feeding, the embryonic STNS generates a rhythm in which the gastric mill and pyloric neurons are all active at about the same frequency (Casasnovas and Meyrand 1995). This has been interpreted as implying that embryonic gastric mill and pyloric neurons are part of a unified rhythmic pattern generator. Fully differentiated and recognizable pyloric and gastric mill rhythms are not clearly evident until metamorphosis from the third larval stage to the first stage of postlarval growth (Casasnovas and Meyrand 1995).

However, does this imply that no features of the gastric mill network are present early in development? Intriguingly, a previous report briefly mentioned that gastric-timed activity was occasionally observed in the output from embryonic gastric mill neurons (Casasnovas and Meyrand 1995). However, to date no attempt has been made to quantify the extent to which gastric mill and pyloric neurons show activity at different frequencies in the embryonic network. To this end, we used spectral methods related to those used previously by Bucher et al. (2006) to analyze long recordings of the output from multiple gastric mill and pyloric neurons. Our results confirmed the earlier finding that embryonic neurons share a common unified frequency, but we also found that gastric mill neurons reliably produced intermittent slow activity reminiscent of the adult gastric mill rhythm. This suggests that an embryonic precursor of the gastric mill rhythm is present even at this early stage of development.

Further support for this idea came from the results of applying a modulator, *Cancer borealis* tachykinin-related peptide 1a (CabTRP), to the embryonic STNS. CabTRP is a neuropeptide found in the neuromodulatory inputs to the STG in adult crabs and lobsters (Blitz et al. 1995; Christie et al. 1997; Goldberg et al. 1988; Thirumalai and Marder 2002). In crabs, CabTRP is found in one of the neurons that activates gastric mill activity (Nusbaum et al. 2001; Wood et al. 2000). Previous work in the isolated STG (with modulatory inputs removed) showed that CabTRP strongly activated some, but not all, neurons in the pyloric network of the lobster, *Homarus americanus* (Thirumalai and Marder 2002). However, the effects of CabTRP on the motor patterns generated by the intact lobster STG (modulatory inputs present) have not been reported. Furthermore, CabTRP appears in the neuromodulatory inputs to the lobster STG late in larval development (Cape et al. 2008; Fénelon et al. 1999). Therefore we compared the effects of CabTRP on the adult and embryonic STNS to ask whether CabTRP would activate gastric mill rhythms similarly at both developmental stages. We found that CabTRP increased the amount of slow activity in gastric mill neurons at both stages. Thus the immaturity of the embryonic neuromodulatory inputs is likely to contribute to the immaturity of the output from the embryonic STNS. Taken together, these results suggest that the STG network can express adult-like rhythmic behavior before fully differentiated adult motor patterns are observed, and that the maturation of neuromodulatory inputs is likely to play a role in the eventual establishment of the adult motor patterns.

METHODS

Adult *H. americanus* (~550–700 g) were purchased from Yankee Lobster (Boston, MA). Embryonic lobsters were harvested from three different egg-bearing lobsters obtained from Dr. M. Tlusty at the New England Aquarium (Boston, MA) and M. Syslo at the Massachusetts State Lobster Hatchery (Martha's Vineyard, MA). Embryos were removed from their egg cases and staged using an eye index according to Helluy and Beltz (1991). Embryos in control saline experiments were 70–99% of embryonic development (E70–E99) and embryos used for the CabTRP experiments were E78–E98. Animals were kept in recirculating artificial seawater tanks at 8–16°C. When indicated, 10^{-6} M CabTRP 1a (gift from Dr. Michael P. Nusbaum, synthesized at the Protein Chemistry Laboratory, University of Pennsylvania, Philadelphia, PA) was bath applied at ~0.05 ml/s using a continuously flowing superfusion system.

Electrophysiological recordings

Adult lobsters were anesthetized on ice for 10–20 min. The stomatogastric nervous system was removed from the stomach and pinned in a Sylgard-coated petri dish and superfused with chilled (10–14°C) saline. Extracellular recordings were obtained using stainless steel pin electrodes placed in petroleum jelly wells around the nerves that contain axons of particular gastric and pyloric neurons: dorsal gastric nerve (dgn) for dorsal gastric (DG); lateral gastric nerve (lgn) for lateral gastric (LG); pyloric dilator nerve (pdn) for pyloric dilator (PD); lateral pyloric nerve (lpn) for lateral pyloric (LP) and medial gastric (MG) (Bucher et al. 2006). Intracellular recordings from identified somata in the STG were made with glass microelectrodes (20–30 M Ω).

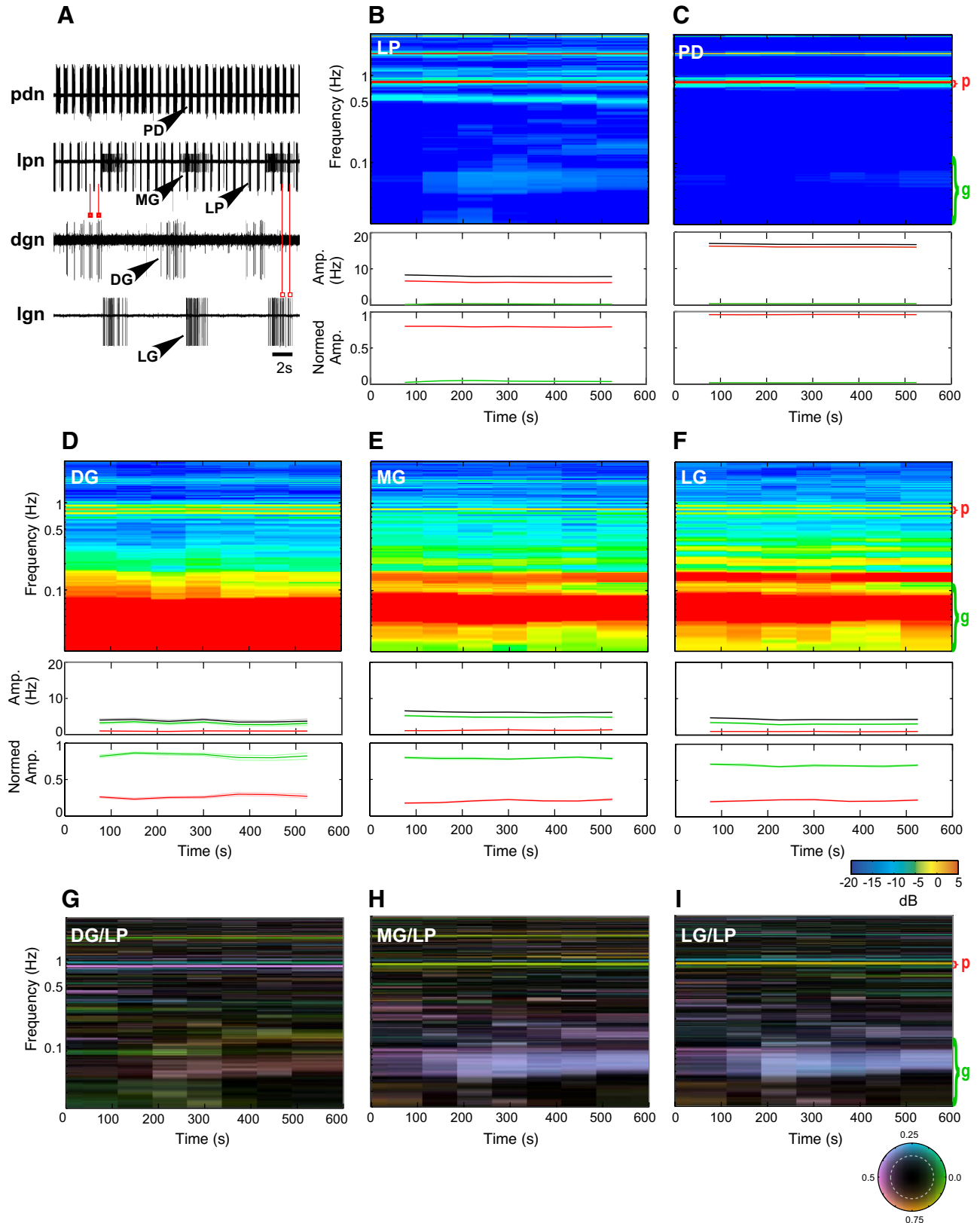
The whole embryo was removed from its egg case and pinned ventral side down in a plastic petri dish coated with a 0.5-cm-thick layer of transparent Sylgard (Dow Corning, Midland, MI; <http://www.dowcorning.com>) with 0.001-gauge tungsten wire (California Fine Wire Company, Grover Beach, CA; <http://www.calfinewire.com>). The carapace and yolk were removed, and a lateral incision was made up the side of the stomach, preserving the PD innervated muscles. The stomach was pinned flat, ventral side down, with 0.0005-gauge tungsten wire and superfused with chilled (10–16°C) saline. It is impossible to remove the STNS from the embryonic stomach; therefore output from embryonic neurons was obtained by intracellular recordings of excitatory junctional potentials (EJPs) from muscles innervated by specific pyloric and gastric mill neurons. Identifications of muscles were made according to Richards (2000). Glass microelectrodes (20–40 M Ω) were used to obtain muscle recordings. LP neuron activity was recorded from either cardio-pyloric valve muscle 6 (cpv6) or pyloric muscle 1 (p1), both of which are innervated by the LP neuron. These two muscles are referred to collectively as lpm. PD neuron activity was recorded from cardio-pyloric valve muscle 2 (cpv2), referred to as pdm; DG neuron activity in gastric mill muscle 4 (gm4), referred to as dgm; LG neuron activity in gastric mill muscle 6 (gm6) or gastric mill muscle 8 (gm8), which we refer to collectively as lgm; and MG neuron activity in gastric mill muscle 9 (gm9), referred to as mgm. Simultaneous recordings from neighboring muscles were made to confirm muscle identification and boundaries between muscles. Recordings ranged from 10 to 110 min (mean = 38 min; median = 33.5 min). In 20% of the recordings, short periods of time (10 s to several minutes) were removed from the analysis because one of the electrode penetrations was lost and recovered. None of these recordings is shown in the figures.

The saline composition was (in mM) 479.12 NaCl, 12.74 KCl, 13.67 CaCl₂, 20 Mg₂SO₄, 3.91 Na₂SO₄, and 5 HEPES; pH, 7.4–7.5. The intracellular microelectrode solution composition

was 0.6 M K_2SO_4 and 20 mM KCl. Signals were amplified by Axoclamp 2B amplifiers (Axon Instruments/Molecular Devices, Sunnyvale, CA; <http://www.moleculardevices.com>) and digitized using a DigiData 1200 data acquisition board (Axon Instruments/Molecular Devices).

Data analysis

Recordings were analyzed with Spike2 (version 5, CED, Cambridge, UK; <http://www.ced.co.uk>) and MATLAB (version 7, The MathWorks, Natick, MA; <http://www.mathworks.com>). Statistical tests



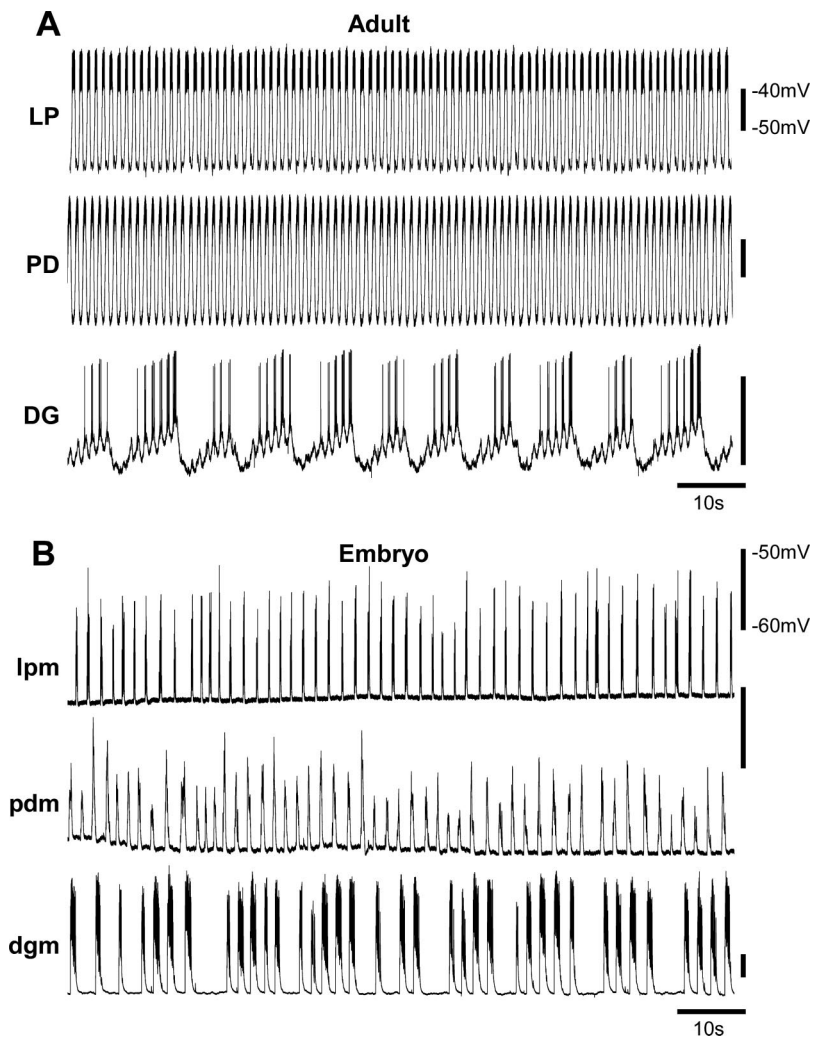


FIG. 2. Adult and embryonic stomatogastric motor patterns. *A*: adult: simultaneous intracellular recordings from somata of LP, PD, and DG neurons. *B*: embryo: simultaneous intracellular recordings from LP-innervated muscles (lpm), PD-innervated muscles (pdm), and DG-innervated muscles (dgm).

and plots were performed in MATLAB and Statview (version 5.0.1, SAS Institute, Cary, NC; <http://www.sas.com>). Figures were created in Canvas (version 10, ACD Systems, Miami, FL; <http://www.acdsee.com>).

Statistics

All error bars represent SE. One-way ANOVAs with Fisher's PLSD post hoc tests were used to compare the mean normed amplitudes in control saline. Unpaired *t*-test and one-way ANOVAs were performed to compare fundamental frequencies and the normed fast and slow amplitudes of the output from two or three neurons, respectively. Unpaired *t*-tests were used to compare the fundamental frequency and the amount of fast and slow activity in embryos and

adults. The Watson-Williams test (Mardia and Jupp 1999) (Igor Pro 6.02A, WaveMetrics, Lake Oswego, OR; <http://www.wavemetrics.com>) was used to compare the coherence phase angles in adults and embryos for each cell type for the control saline experiments. Paired *t*-tests were used to compare the fundamental frequencies in control and CabTRP. To test whether changes in coherence phase angle caused by CabTRP application were significant, we used a circular analog of the paired *t*-test (Mardia and Jupp 1999; Upton 1973).

Spectral analysis

The adult STG generates two distinct rhythms, as seen in the extracellular nerve recordings in Fig. 1A. The faster pyloric rhythm,

FIG. 1. Pyloric and gastric mill rhythms in the stomatogastric motor patterns of the adult lobster. *A*: simultaneous extracellular recordings from gastric mill and pyloric nerves. Top trace, pyloric neuron pyloric dilator (PD) activity in the pyloric dilator nerve (pdn) recording. Second trace, pyloric neuron lateral pyloric (LP) and gastric mill neuron medial gastric (MG) activity in the lateral pyloric nerve (lpm). Third trace, gastric mill neuron dorsal gastric (DG) activity in the dorsal gastric nerve (dgn). Fourth trace, gastric mill neuron lateral gastric (LG) activity in the lateral gastric nerve (lgn). Pyloric-timed events within each DG burst (red closed boxes) occurred between each LP burst. Pyloric-timed events within each LG burst (red open boxes) were synchronized with LP bursting. *B–F*: spectrograms (bin size = 160 s) and graphs of amplitude (square root of power) of activity of pyloric neurons LP and PD (*B* and *C*) and gastric mill neurons DG, MG, and LG (*D–F*) over the entire 10-min recording. Color scale indicates amplitudes in decibels, equal to $10 \cdot \log_{10}(P)$, where *P* is the normalized power density (see METHODS). Pyloric frequencies are indicated with a red bracket, and gastric mill frequencies are indicated with a green bracket. The plot directly below each spectrogram shows the total amplitude (black line), amplitude of pyloric activity (red line), and the amplitude of gastric mill activity (green line). The 2nd plot below each spectrogram shows the amplitude of pyloric (red line) and gastric mill activity (green line) normalized to the total amplitude. In the amplitude and normed amplitude plots, the *x*-coordinate of each point is the center of the window for which it was calculated, so the 1st and last points are one half the window duration away from the edges of the plot (see METHODS). *G–H*: coherograms of activity between DG and LP (*G*), MG and LP (*H*), and LG and LP (*I*). The relationship between coherence and color is shown in the inset circle. Each possible coherence value corresponds to a point in a circle of radius 1 (see METHODS). The dashed circle in the inset indicates the threshold for statistical significance of the coherence magnitude. Recordings courtesy of Dirk Bucher.

which typically has a frequency of ~ 1 Hz, is expressed by the PD and LP neurons, as seen in the nerve recordings pdn and lpn, respectively. The gastric mill rhythm, typically ~ 0.1 Hz, is seen as activity in the DG (dgn), LG (lgn), and MG (lpn) neurons (Fig. 1A). A cell can participate in both rhythms simultaneously, resulting in an activity pattern that includes both fast (pyloric) and slow (gastric) bursting. This can be seen in the recordings of the adult DG and LG neurons, in which there are pyloric-timed events within each slow gastric burst (Fig. 1A).

We used spectral analysis to examine the variation in a neuron's spike rate at different frequencies. All spectral analysis was done using custom Matlab scripts. To convert extracellular nerve recordings to a spike train, we used a simple threshold-crossing algorithm. To convert intracellular muscle recordings to a spike train, we first high-pass filtered the signal, followed by a threshold-crossing algorithm. The high-pass filter involved subtracting off a moving-window average of the original signal, using a rectangular window of width typically ~ 40 ms. Spurious threshold crossings were eliminated by deleting any crossings that occurred < 20 ms after the previous

crossing. The spike trains were converted to a continuous rate-versus-time signal, $r(t)$, by filtering the spike train (interpreted as a train of impulses) with a Gaussian filter ($\sigma = 50$ ms). The continuous signal $r(t)$ was "sampled" at a rate of 250 Hz. These signals appeared by eye to be a reasonable representation of the gastric-like and pyloric-like modulation of the spike rate.

To examine how the frequency content of the signals varied over time, we calculated spectrograms of the signals by dividing the signal into a number of temporal windows and estimating the power spectrum for each window (Thomson 2000). The power spectrum is a representation of how much of the variation in a signal can be accounted for by variation at different frequencies and is equal to the Fourier transform of the autocorrelation function of the signal. When a large amount of the variation in a signal can be accounted for by variation at a particular frequency, there is a lot of "power" at that frequency. The spectrogram therefore shows which frequencies contribute to a signal over time.

We estimated the power spectrum for each window using multi-taper spectral estimation (Percival and Walden 1993), using windows

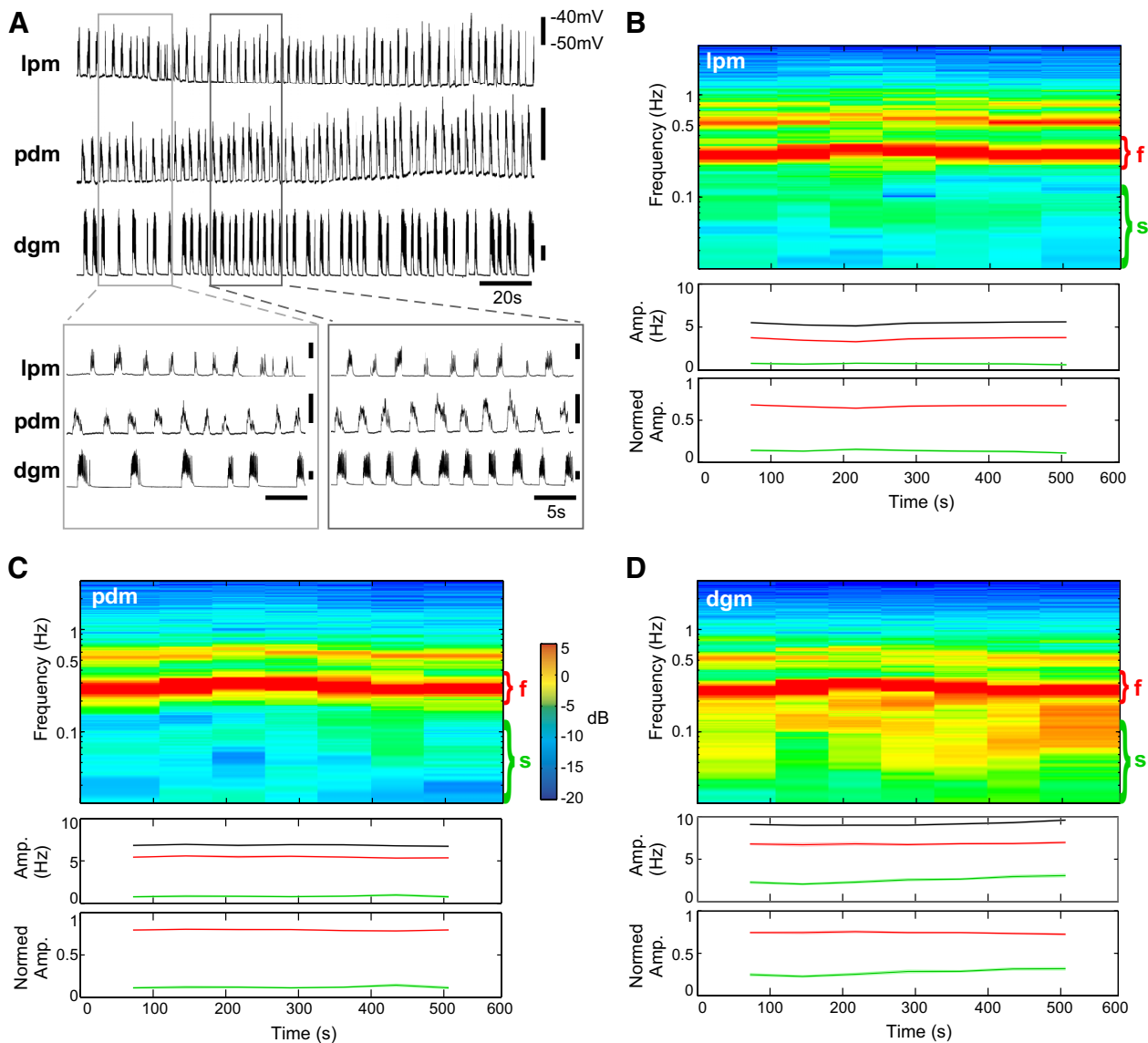


FIG. 3. Activity in embryonic lpm, pdm, and dgm. *A*: simultaneous intracellular recordings from lpm, pdm, and dgm muscles. *B–D*: spectrograms of activity in lpm (*B*), pdm (*C*), and dgm (*D*) over the entire 10-min recording. Below each spectrogram, amount of activity in embryonic-fast (red bracket on each spectrogram) and embryonic-slow (green bracket on each spectrogram) frequency ranges are plotted as amplitude and normed amplitude lines of the embryonic-fast (red lines) and embryonic-slow (green lines) activity.

of length $T \approx 160$ s (range, 138.9–169.7 s) for the control saline experiments and $T \approx 100$ s (range, 91.7–112.7 s) for the CabTRP experiments. The frequency resolution of the spectrum is chosen by picking a value for the time-bandwidth product (denoted NW). Given a time-bandwidth product, the frequency resolution of the estimated spectrum is $2NW/T$. The per-window spectrum estimate was calculated using $NW = 4$, yielding a frequency resolution of ~ 0.05 Hz (range, 0.047–0.058 Hz) for the control experiments and ~ 0.08 Hz (range, 0.07–0.09 Hz) for the CabTRP experiments. Seven tapers were used, and the estimates for each taper were averaged together within each window. The amount of window overlap was 50%, so that the last half of one window was the same as the first half of the next.

All spectrograms were normalized as follows. For each window, the total power was computed by integrating the power across frequencies. The average of the total power was then taken (across windows). All points of the spectrogram were divided by the mean total power to yield the normalized spectrogram. The raw spectrogram has units of Hz^2/Hz whereas the normalized spectrogram has units of $1/\text{Hz}$. The normed spectrogram was converted to decibels by taking the logarithm (base 10) of the normalized spectrogram and multiplying by 10. The normalized spectrogram in decibels (dB) was plotted.

Figure 1, *B–F*, shows spectrograms calculated from the activity of the LP, PD, DG, MG, and LG neurons shown in Fig. 1A. Power is represented by color, where colors toward the blue end of the spectrum indicate low power, and colors toward the red end of the

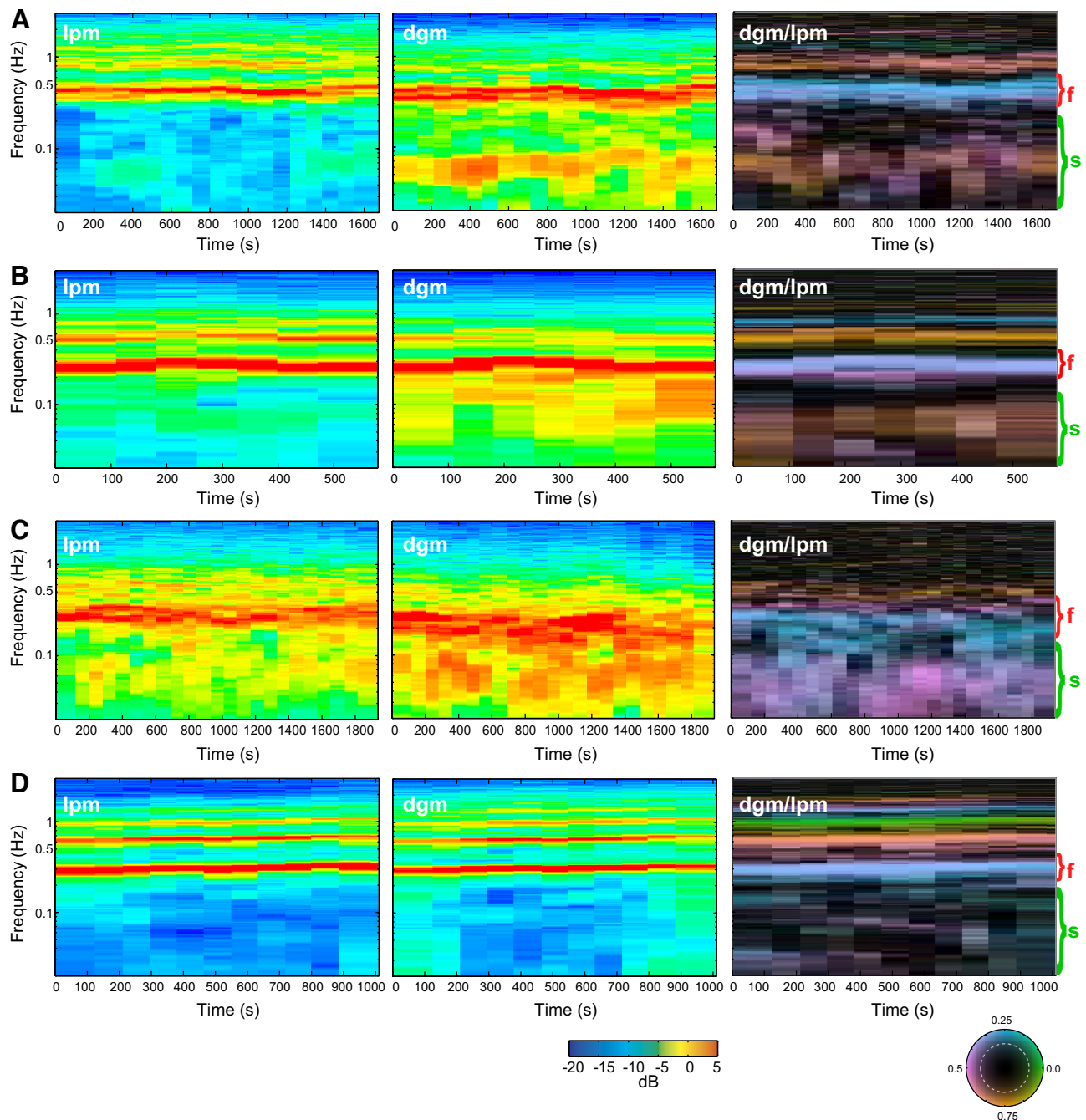


FIG. 4. Spectrograms of lpm and dgm activity in 4 embryonic preparations. *A–D*: spectrograms of activity from simultaneous lpm and dgm recordings in 4 embryonic preparations. Lpm spectrograms, *left*; dgm spectrograms, *middle*; dgm/lpm coherograms, *right*.

spectrum indicate high power. The red areas in the spectrograms of the LP and PD neurons are at 0.94 Hz, the frequency of the pyloric rhythm (Fig. 1, *B* and *C*), whereas the red areas in the spectrograms of the DG, MG, and LG neurons are at 0.11 Hz, the frequency of the gastric mill rhythm (Fig. 1, *D–F*).

To quantify the amount of power in the pyloric and gastric frequency ranges (red and green brackets on the spectrograms in Fig. 1, *C* and *F*), we first plotted the amplitude (square root of power) of the total activity (black line) and the amplitude of activity in the gastric (green line) and pyloric (red line) frequency ranges (Fig. 1, *B–F*, 1st plot below each spectrogram). We normalized the amplitude in each frequency range to the total amplitude and plotted these over time (Fig. 1, *B–F*, 2nd plots below each spectrogram). In these plots, the *x*-coordinate of each point is the center of the window for which it was calculated, so the first and last points are one half the window duration away from the edges of the plot. CIs on these estimates were calculated using the jackknife estimate of SE, by performing take-away-one estimates of the logarithm (base 10) of amplitude and normed amplitude and using the percentiles of a *t* distribution with $n_{\text{tapers}} - 1$ degrees of freedom to calculate an approximate 68% CI (Thomson and Chave 1991).

In the power spectra, rhythmic activity appeared as a peak at the fundamental frequency of the rhythm and also as harmonics at integer multiples of this frequency. Pyloric and gastric frequency ranges were chosen by eye to include the peak power at the fundamental frequency and to exclude the harmonics. To calculate the pyloric frequency, we first estimated an overall power spectrum for each spectrogram (data not shown) by averaging together the power spectra for every other window used in the spectrogram (so that the windows were not overlapping). To determine the frequency of the fundamental, we found the frequency with maximum power density from the relevant frequency range.

Coherence

To calculate the extent to which spiking activity in two signals was correlated as a function of frequency, we divided the data into the same number of temporal windows as for calculating spectrograms and estimated the normalized cross-spectrum (called the coherence) of the two signals in each window. The coherence is a complex-valued quantity, having both a magnitude and a phase at each frequency. The magnitude reflects the extent to which the variations in the two signals are correlated at the given frequency, and the phase reflects the extent to which one leads or lags the other. The coherence magnitude can take on values between 0 and 1, 0 indicating no correlation and 1 indicating perfect correlation.

Estimation of coherence was also done using the multitaper technique, with the same window lengths, time-bandwidth product, and number of tapers as above. The coherence magnitude was considered significantly different from 0 when it exceeded $\sqrt{1 - \alpha^{1/(2NW-2)}}$ for $\alpha = 0.05$ (Jarvis and Mitra 2001).

The coherograms in Fig. 1, *G–I*, show the frequencies at which there is coherent activity in the two indicated neurons and the phase relationship of that coherent activity over time. The coherograms show the coherence as a function of both time (*x*-axis) and frequency (*y*-axis), with coherence coded by color. Bright colors represent high coherence magnitude, and the particular hue indicates the phase of the coherence. Dark colors indicate low coherence. In the legend, the coherence phase is given as a fraction of a cycle, with a phase of 0 indicating synchronous activity and a phase of 0.5 indicating alternating activity. When calculating coherence, one signal is used as a reference, and the phase is that of the other signal (the “query” signal) relative to the reference signal. Thus a coherence phase of 0.25 means that the peak of the query signal occurred a quarter cycle after that of the reference signal (at the frequency in question). When describing a particular coherence estimate, we describe the estimate as query/reference. For instance, Fig. 1*G* shows a coherogram of DG and LP, with DG used as the query and LP used as the reference (thus it is labeled DG/LP, not LP/DG).

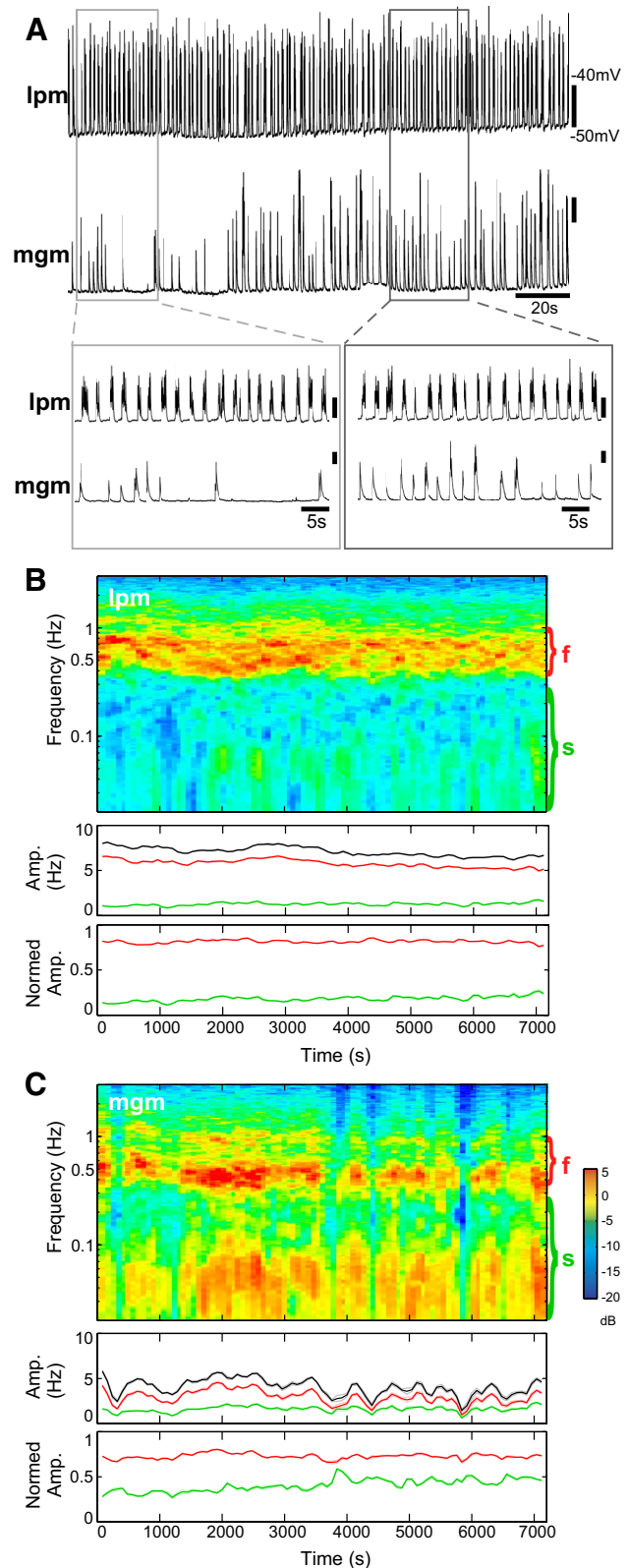


FIG. 5. Activity in embryonic lpm and mgm. *A*: simultaneous intracellular recordings from lpm and mgm muscles. *B* and *C*: spectrograms and amplitude of activity in lpm (*B*) and mgm (*C*) over the entire 110-min recording.

Estimation of coherence phase for whole traces

To estimate the relative phase of cells displaying pyloric activity, we used the phase of the coherence between the two cells. We collapsed the coherogram into a single coherence spectrum by averaging the complex coherence spectra for each window used in the coherogram. (To be precise, we averaged the coherence spectra from every *other* window, so that the windows were not overlapping.) Using the mean coherence spectrum (data not shown), we identified the frequency within the pyloric band that had the maximum coherence magnitude. We call this the peak coherence phase and use it as an estimate of the phase of one cell relative to the other for the pyloric-like activity. These estimates were in qualitative agreement with visual inspection of the data traces.

RESULTS

Adult and embryonic motor patterns

Figure 2 provides example recordings from adult LP, PD, and DG neurons (Fig. 2A) and from muscles innervated by those neurons—lpm, pdm, and dgm—in an embryo (Fig. 2B). In the adult, the LP and PD neurons are rhythmically active in the pyloric rhythm, and the DG neuron is active in the slower gastric mill rhythm. Note that, although the DG neuron is firing in long, slow, gastric-timed bursts, its activity is also modulated by the faster pyloric rhythm (Bucher et al. 2006). This is seen as the pyloric-timed interruptions during the DG neuron firing, as well as

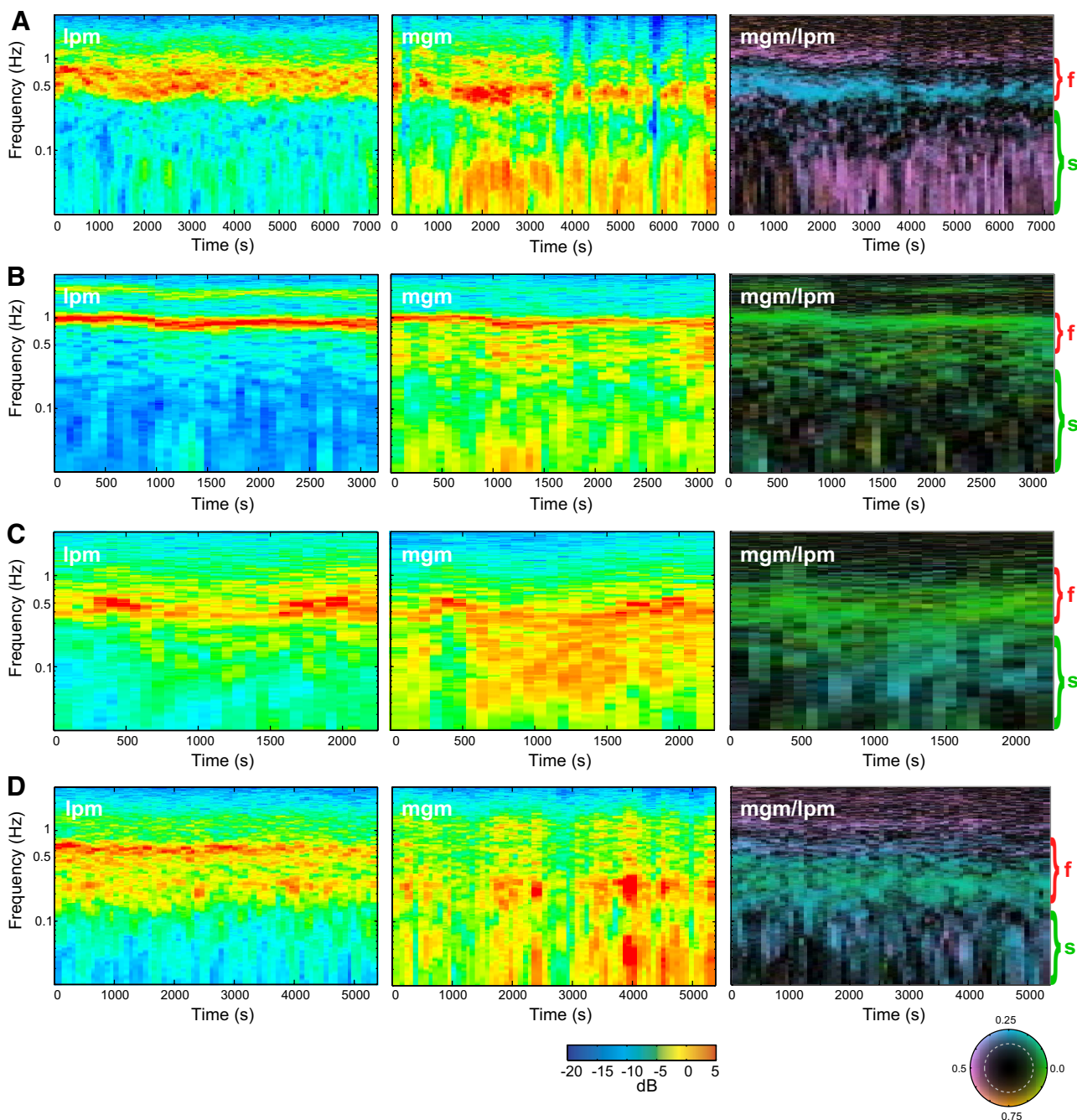


FIG. 6. Spectrograms of lpm and mgm activity in 4 embryonic preparations. A–D: spectrograms of activity from simultaneous lpm and mgm recordings in 4 embryonic preparations. Lpm spectrograms, left; mgm spectrograms, middle; mgm/lpm coherograms, right.

pyloric-timed subthreshold activity when the DG neuron is silent. In these data, as is typical in the adult, there is a clearly defined pyloric rhythm and a clearly defined and separate gastric mill rhythm.

The clean separation of pyloric and gastric activity seen in the adult contrasts with the situation in the embryo (Fig. 2*B*). Previous studies have reported that embryonic pyloric and gastric mill neurons burst at a common frequency (Casasnovas and Meyrand 1995), one that is slower and less regular than the adult pyloric frequency (Richards et al. 1999). Consistent with these results, the common rhythm in embryonic lpm and pdm was slower than the adult pyloric rhythm. In contrast to previous reports (Casasnovas and Meyrand 1995; Ducret et al. 2007; Le Feuvre et al. 1999), we reliably observed pauses in the dgm recordings, in which dgm failed to fire in time with the bursts in lpm and pdm (Fig. 2*B*). These pauses were reminiscent of the gastric-timed DG pauses observed in the adult (Fig. 2*A*). This suggests that these pauses might be precursor of the adult gastric mill rhythm, and the common embryonic rhythm might be a precursor of the adult pyloric rhythm. In contrast with the adult, however, the gastric-like activity did not always have one regular, clearly defined frequency; thus we call this “embryonic-slow activity.” Similarly, to distinguish the common embryonic rhythm from the adult pyloric rhythm, we call it the “embryonic-fast rhythm” (Fig. 2*B*).

Spectral analysis of adult motor patterns

The pyloric and gastric mill rhythms in adult lobsters and crabs have been extensively analyzed using traditional burst analyses that measure the period of the rhythm, the relative phase of firing of each neuron, and the duty cycle of each neuron (Bucher et al. 2005; Selverston and Moulins 1987). Embryonic motor patterns are often irregular, however, making burst detection difficult or impossible (Richards et al. 1999). Consequently, we used spectral techniques that do not depend on burst detection to analyze both adult and embryonic motor patterns in both control saline and in the presence of the neuropeptide CabTRP.

Figure 1 shows the use of spectrograms and coherograms to describe the activity of adult pyloric and gastric network neurons. Figure 1*A* shows the extracellular traces used to calculate the spectrograms. Spectrograms of activity in adult LP and PD neurons displayed high power at the pyloric frequency and low power at the gastric mill frequency, and spectrograms of activity in adult DG, MG, and LG neurons displayed high power at the gastric mill frequency and low power at the pyloric frequency (Fig. 1, *B–F*, top subpanels). These features are reflected in both the raw and normed amplitude in the pyloric and gastric mill bands: pyloric neurons have high pyloric amplitude and low gastric mill amplitude, and gastric mill neurons have high gastric mill amplitude and low pyloric amplitude (Fig. 1, *B–F*, bottom subpanels). Rhythmic activity in the adult was regular and stable over time; the high-power bands in all of the spectrograms (Fig. 1, *B–F*, top subpanel) are horizontal, and the power remains constant along the band. Similarly, the amplitude lines in the graphs below each spectrogram are all horizontal (Fig. 1, *B–F*, bottom subpanels).

Coherograms provide information about the relative phase at which different neurons are active. The brightest band in the DG/LP coherogram (Fig. 1*G*) is a narrow horizontal band at the pyloric frequency, indicating that the DG neuron exhibits a stable phase relationship with the LP neuron at the pyloric frequency.

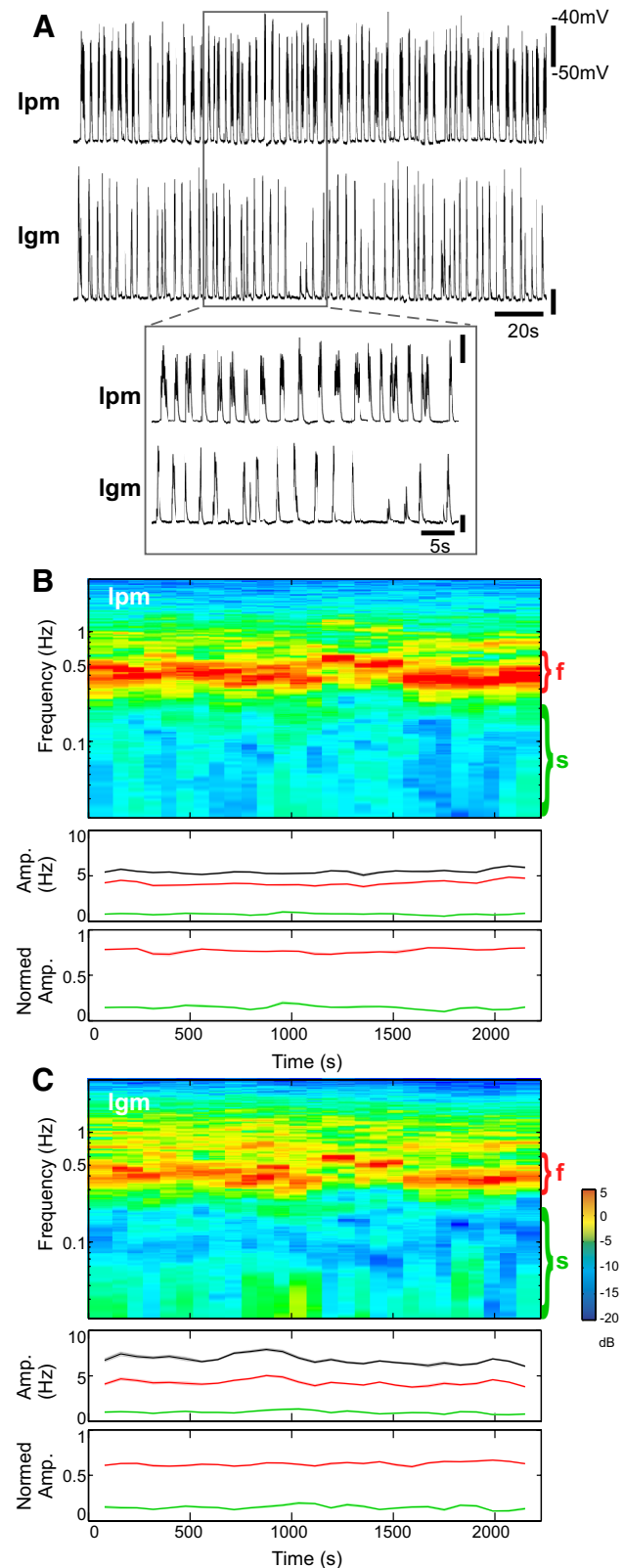


FIG. 7. Activity in embryonic lpm and lgm. *A*: simultaneous intracellular recordings from lpm and lgm muscles. *B* and *C*: spectrograms and amplitude of activity in lpm (*B*) and lgm (*C*) over the entire 40-min recording.

The LP and DG neurons burst in alternation and have a peak coherence phase of 0.5, consistent with the raw traces of LP and DG neuron activity (Fig. 1A). There is also stable coherent activity between the LP and MG neurons (Fig. 1H) and the LP and LG neurons (Fig. 1I), as shown by the horizontal bands at the pyloric frequency in these coherograms. These bands are at peak coherence phases of ~ 0.1 for MG/LP and ~ 0.2 for LG/LP, indicating that pyloric-timed activity in MG and LG occurs almost synchronously with LP bursting. These phase relationships are consistent with the apparent phasing seen in the traces and with traditional methods of estimating the phase relationships.

Pyloric neurons can also have gastric-timed activity, a phenomenon reported in the adult STNS (Bucher et al. 2006;

Mulloney 1977; Weimann et al. 1991). This slow activity, seen dimly at ~ 0.1 Hz in the LP spectrogram (Fig. 1B), is coordinated with the slow activity in MG (Fig. 1H) and LG (Fig. 1I). The low-frequency bands in the MG/LP and LG/LP coherograms are not as bright and straight and have more color changes than the higher frequency bands, indicating that, at least in this example, the slow coherent MG/LP and LG/LP activity is less stable than the fast coordinated activity (Fig. 1, H and I).

Fast and slow components of the embryonic motor pattern

Unlike adult rhythms that can be stably expressed for long periods of time (Fig. 1A), embryonic preparations often showed considerable activity variation, as seen in the re-

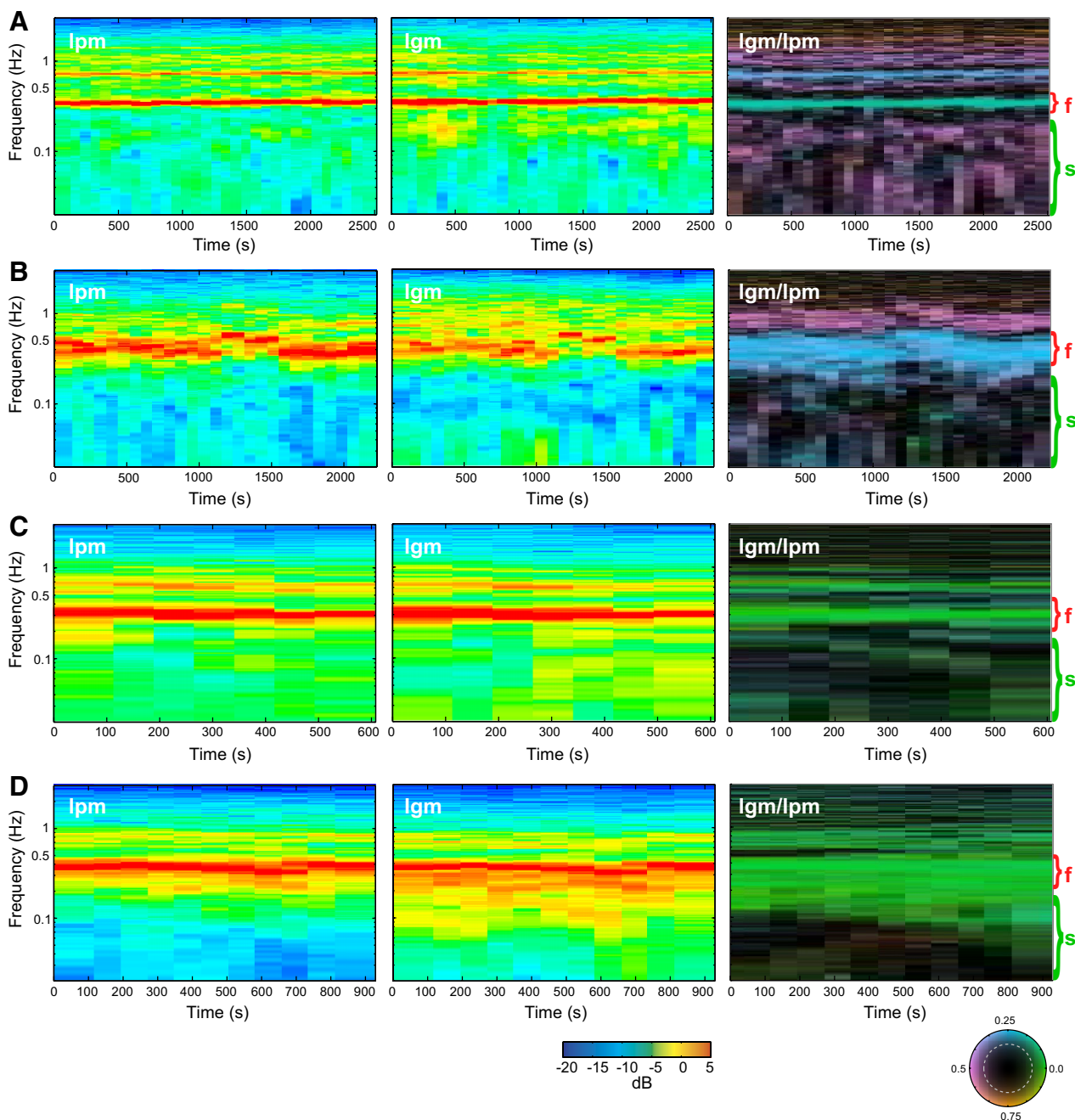


FIG. 8. Spectrograms of lpm and lgm activity in 4 embryonic preparations. A–D: spectrograms of activity from simultaneous lpm and lgm recordings in 4 embryonic preparations. Lpm spectrograms, left; lgm spectrograms, middle; lgm/lpm coherograms, right.

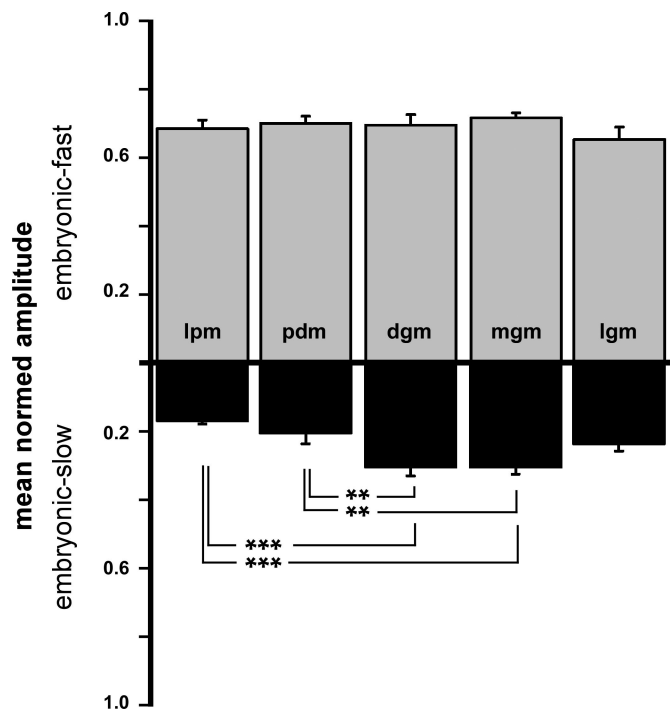


FIG. 9. Mean normed amplitudes of fast and slow activity in the embryo. Mean normed amplitudes of the embryonic-fast (gray) and embryonic-slow (black) activity in embryonic lpm ($n = 25$), pdm ($n = 10$), DG ($n = 13$), mgm ($n = 10$), and lgm ($n = 5$). There were significant differences in the amplitude of slow activity across embryonic neurons (1-way ANOVA, $P < 0.0001$): mgm and dgm showed more slow activity than lpm (Fisher's PLSD post hoc tests, $P < 0.0001$); dgm showed more slow activity than pdm (Fisher's PLSD, $P = 0.001$); and mgm showed more slow activity than pdm (Fisher's PLSD, $P = 0.003$). lgm tended to show more slow activity than lpm (Fisher's PLSD, $P = 0.06$) and less slow activity than dgm (Fisher's PLSD, $P = 0.052$) and mgm (Fisher's PLSD, $P = 0.08$). There were no significant differences in the amount of slow activity between dgm and mgm, lpm and pdm, and pdm and lgm (Fisher's PLSD, $P > 0.16$). There were no significant differences in the amount of fast activity across cell types (1-way ANOVA, $P = 0.80$). Asterisks indicate significant differences: ** $P < 0.01$, *** $P < 0.001$.

cordings from embryonic lpm, pdm, and dgm (Fig. 3A). Furthermore, although activity in embryonic lpm, pdm, and dgm appear to have the same burst frequency for some periods of time (Fig. 3A, 2nd inset), there were intermittent pauses in dgm activity that were not apparent in the recordings from lpm and pdm (Fig. 3A, 1st inset).

In the spectrograms of lpm, pdm, and dgm activity (Fig. 3, B–D), the highest-power band is in the embryonic-fast frequency range; most of the activity from all three neurons occurred at this frequency (~ 0.3 Hz). However, there is also significant power at lower frequencies in the lpm spectrogram (< 0.14 Hz), arising from the pauses of different lengths that occurred in the dgm recording (Fig. 3D, within green bracket). For all three cells, the normed amplitude in the embryonic-fast rhythm frequency range is higher than that in the embryonic-slow activity frequency range (Fig. 3, B–D, bottom graph in each panel). However, the mean normed amplitude in the embryonic-slow frequency range is more than twofold higher in dgm (0.276 ± 0.033) than in lpm (0.137 ± 0.019) and pdm (0.114 ± 0.005). This embryonic-slow activity in dgm is less stable than activity in the higher frequency range; the embryonic-fast band in the dgm spectrogram has higher power, is

narrower (even when viewed on a linear scale) and is more nearly horizontal (Fig. 3D).

In all preparations ($n = 10$) in which simultaneous lpm, pdm, and dgm recordings were obtained, there was more slow activity in dgm as compared with the lpm and pdm. This is shown in the spectrograms of simultaneous lpm and dgm recordings from four representative preparations (Fig. 4). In all dgm/lpm experiments, there was slow activity in the dgm spectrogram that was not present in the lpm spectrogram from the same preparation. This slow activity appeared as a bright, low-frequency band that was clearly separate from the fast activity band in some of the dgm spectrograms (Fig. 4A, traces in Fig. 2B, and in three additional preparations; data not shown). However, in most cases, the pauses in dgm were quite irregular. This appears

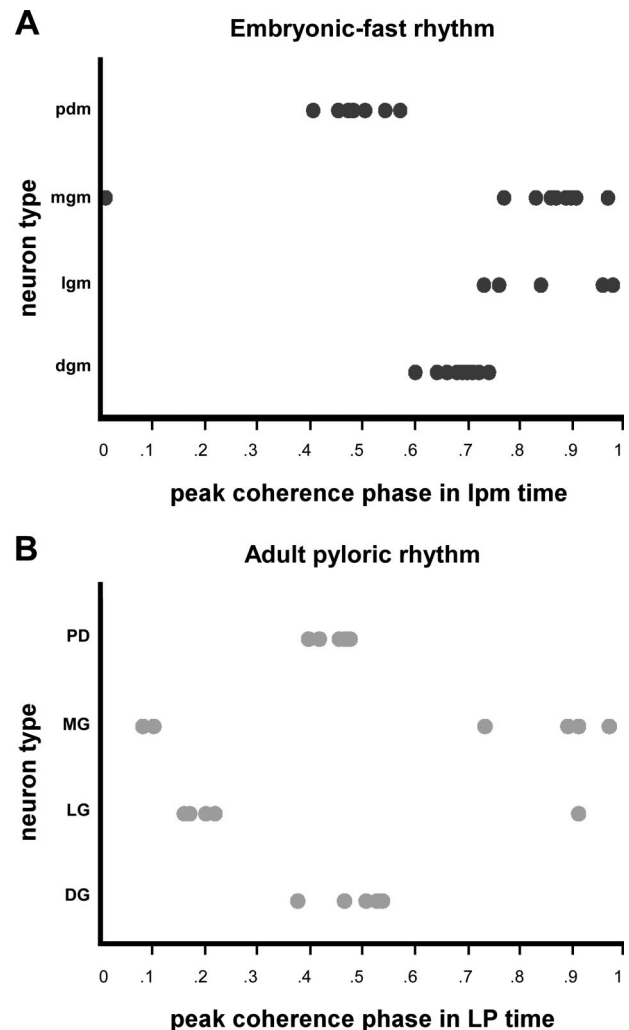


FIG. 10. Phase relationships of embryonic-fast activity and adult pyloric activity. Peak coherence phase of the fast activity in each neuron with respect to LP. A: phase relationships of embryonic-fast activity in lpm and pdm (mean phase, 0.49 ± 0.05 ; $n = 10$), mgm (mean phase, 0.80 ± 0.28 ; $n = 10$), lgm (mean phase, 0.86 ± 0.11 ; $n = 5$), and dgm (mean phase, 0.69 ± 0.04 ; $n = 10$). B: phase relationships of pyloric activity in adult LP and PD (mean phase, 0.45 ± 0.03 ; $n = 5$), MG (mean phase, 0.62 ± 0.42 ; $n = 6$), LG (mean phase, 0.31 ± 0.30 ; $n = 5$), and DG (mean phase, 0.48 ± 0.06 ; $n = 6$). Statistical differences were found between embryos and adults in the peak coherence phase of activity produced by DG/LP (Watson-Williams test, $P < 10^{-7}$) and LG/LP (Watson-Williams test, $P < 0.01$). These data come from 7 adult preparations previously reported (Bucher et al. 2006) and 7 adult preparations reported here for the first time.

in the spectrograms as diffuse power at frequencies below the embryonic-fast frequency (Fig. 4, *B* and *C*). In still other preparations, slow dgm activity was minimal (Fig. 4*D* and two additional preparations; data not shown). In all dgm recordings, the fast activity was more stable over time than the slow activity (Fig. 4, *A–D*). Nevertheless, the majority of embryonic dgm recordings displayed some amount of embryonic-slow activity.

In the coherograms of lpm and dgm (Fig. 4, *A–D*, right column), the most obvious band of coordinated activity is found in the embryonic-fast frequency range. The phase relationship of the coherent fast activity was very similar from preparation to preparation, suggesting that the embryonic-fast activity common to lpm and dgm has a stable phase relationship. This coherent band at high frequencies had a phase between 0.5 and 0.75 in most preparations, indicating that when dgm and lpm fired at a common fast frequency, dgm fired either midway between lpm bursts or somewhat later. As in the adult, there was less coherence between dgm and lpm for embryonic-slow frequencies than for the embryonic-fast frequencies, which is further evidence that most of the embryonic-slow activity was unique to dgm (Fig. 4, *A*, *B*, and *D*). The phase of this coherent slow activity was also less consistent than that of the coherent activity in the high-frequency range (Fig. 4, *A*, *B*, and *D*). Thus the fast motor pattern common to embryonic lpm and dgm was more substantial and had a more stable phase relationship than the slower activity common to lpm and dgm.

Activity expressed by other gastric mill neurons

Embryonic mgm also showed substantial embryonic-slow activity in five of five of preparations. The pauses in mgm activity were more pronounced than those in dgm (Fig. 5*A*). As with dgm, these pauses occurred intermittently, with no clear temporal pattern. The spectrograms for lpm and mgm both show a band of activity at ~ 0.5 Hz, corresponding to the embryonic-fast rhythm (Fig. 5, *B* and *C*). Additionally, the mgm spectrogram has substantial power at frequencies < 0.3 Hz (Fig. 5, *B* and *C*). This low-frequency activity is separate from the embryonic-fast band and has peak power as high as that of the embryonic-fast band (Fig. 5*C*). The mean normed amplitude of the embryonic-slow activity in mgm (0.406 ± 0.067) is more than two times higher than that in lpm (0.181 ± 0.030). Overall, mgm activity is less stable than lpm activity—there are more variations in power in the mgm spectrogram compared with the lpm spectrogram.

Figure 6 shows the activity in embryonic lpm and mgm across four representative preparations. There is substantial low-frequency power in all four mgm spectrograms that is absent from the lpm spectrograms (Fig. 6, *A–D*). As in dgm, the slow activity in mgm was intermittent. In all preparations, there is nearly as much low-frequency power as high-frequency power at times (Fig. 6, *A*, *C*, and *D*), and in three preparations, the low-frequency power is well-separated from the high-frequency power (Fig. 6, *A*, *B*, and *D*). The slow activity in mgm was not stable, as there are frequent and dramatic variations in power in the slow activity band (Fig. 6, *A–D*). Although there are variations in power in the high-frequency band of the mgm spectrograms, this variability is less pronounced than that in the low-frequency range (Fig. 6, *B–D*). In contrast, activity in the lpm spectrograms was much more stable across time (Fig. 6, *A–D*).

In lpm and mgm, there was more obvious coordinated activity in the embryonic-fast frequency range compared with the embryonic-slow frequency range. In the mgm/lpm coherograms, coordination appears as a horizontal band of constant phase at the embryonic-fast rhythm frequency (Fig. 6, *A–D*). This coherent band has a phase near 0 in all but one preparation (Fig. 6*A*), indicating that at this frequency lpm and mgm fired synchronously (Fig. 6, *B–D*). The embryonic-slow coherent band is often not a clear, separate band as it is in the mgm spectrogram and appears as an extension of the pyloric band (Fig. 6, *B–D*). As with lpm and dgm, the phase relationship of the slow activity in lpm and mgm activity was less stable than the phase relationship of the fast activity (Fig. 6, *B–D*).

Figure 7 shows one example recording from lgm. In this preparation, pauses in lgm activity were rare (Fig. 7*A*). Consistent with this, the spectrograms show that the frequency content of lpm and lgm was similar over the length of these recordings (Fig. 7, *B* and *C*). The power at all frequencies fluctuated more in lgm than in lpm (Fig. 7, *B* and *C*), suggesting that lgm activity was less stable than lpm activity in this preparation.

The embryonic-fast rhythm (~ 0.5 Hz) predominated in the spectrograms of lpm and lgm recordings from four different preparations (Fig. 8, *A–D*). The embryonic-fast rhythm was strong and stable over time, whereas embryonic-slow activity was weak. In three of these four preparations, activity in dgm was also recorded (data not shown). In all of these preparations, there appeared to be more slow activity in the

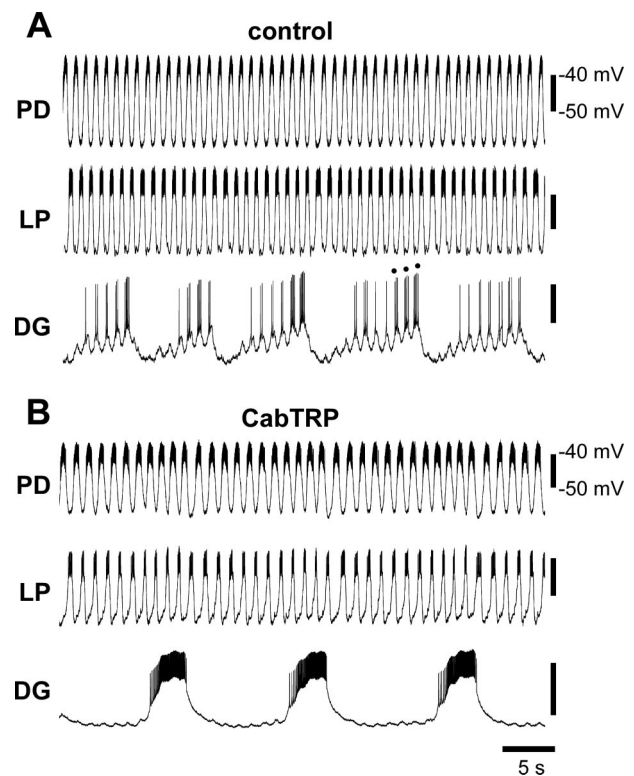


FIG. 11. Adult LP, PD, and DG activity in control saline and in *Cancer borealis* tachykinin-related peptide (CabTRP). Simultaneous intracellular recordings from adult PD, LP, and DG neurons. *A*: in control saline. Closed circles above 3 example pyloric-timed events within a slow, gastric-timed burst of DG. *B*: in 10^{-6} M CabTRP.

dgm spectrograms compared with the lgm spectrograms, although these differences were not significant (unpaired *t*-test, $P = 0.32$; mean normed slow amplitude lgm = 0.23 ± 0.06 ; mean normed slow amplitude dgm = 0.31 ± 0.13).

As with dgm/lpm (Fig. 4) and mgm/lpm (Fig. 6), most of the coherent activity in the lgm/lpm coherograms occurred in the embryonic-fast frequency range (~ 0.5 Hz). This coordinated fast activity was stable (Fig. 8, A–D). The embryonic lgm and lpm fired synchronously at the common embryonic-fast frequency (Fig. 8, A, C, and D). There was little coordinated slow activity in the lgm/lpm coherograms, and whatever coherence was present had no clearly defined phase relationship (Fig. 8, A–D).

Summary of embryonic and adult motor patterns

Figure 9 shows the summary of the mean normed amplitudes of the embryonic-fast and embryonic-slow activity in all recordings. The majority of the power in the output from all neurons was in the embryonic-fast frequency range regardless of cell type. Nevertheless, there was significantly more embryonic-slow activity in both dgm and mgm as compared with lpm and pdm (Fig. 9, statistics in figure legend). lgm appeared to have more embryonic-slow activity than lpm and pdm and less

than both mgm and dgm, but these differences were not statistically significant (Fig. 9, statistics in figure legend).

We also compared the amount of fast and slow activity in embryos and adults. There was more fast activity in adult LP and PD neurons compared with embryonic lpm and pdm (adult LP: mean normed pyloric amplitude = 0.86 ± 0.05 ; embryonic lpm: mean normed fast amplitude = 0.68 ± 0.11 ; adult PD: mean normed pyloric amplitude = 0.90 ± 0.06 ; embryonic pdm: mean normed fast amplitude = 0.70 ± 0.05 ; unpaired *t*-test, $P < 0.001$; adult LP and PD, $n = 7$; embryonic lpm, $n = 25$; embryonic pdm, $n = 10$) and less slow activity in adults compared with embryos (adult LP: mean normed gastric amplitude = 0.06 ± 0.03 ; embryonic lpm: mean normed slow amplitude = 0.17 ± 0.05 ; adult PD: mean normed gastric amplitude = 0.04 ± 0.02 ; embryonic pdm: mean normed slow amplitude = 0.21 ± 0.09 ; unpaired *t*-test, $P < 0.001$; adult LP and PD, $n = 7$; embryonic lpm, $n = 25$; embryonic pdm, $n = 10$). There was more slow activity in adult DG neurons compared with embryonic dgm (adult DG: mean normed gastric amplitude = 0.50 ± 0.22 ; embryonic dgm: mean normed slow amplitude = 0.31 ± 0.09 ; unpaired *t*-test, $P < 0.001$; adult, $n = 7$; embryo, $n = 13$) and no significant difference in the amount of fast activity between embryonic dgm and adult DG (adult DG: mean normed pyloric amplitude = 0.63 ± 0.23 ; embryonic dgm: mean normed fast

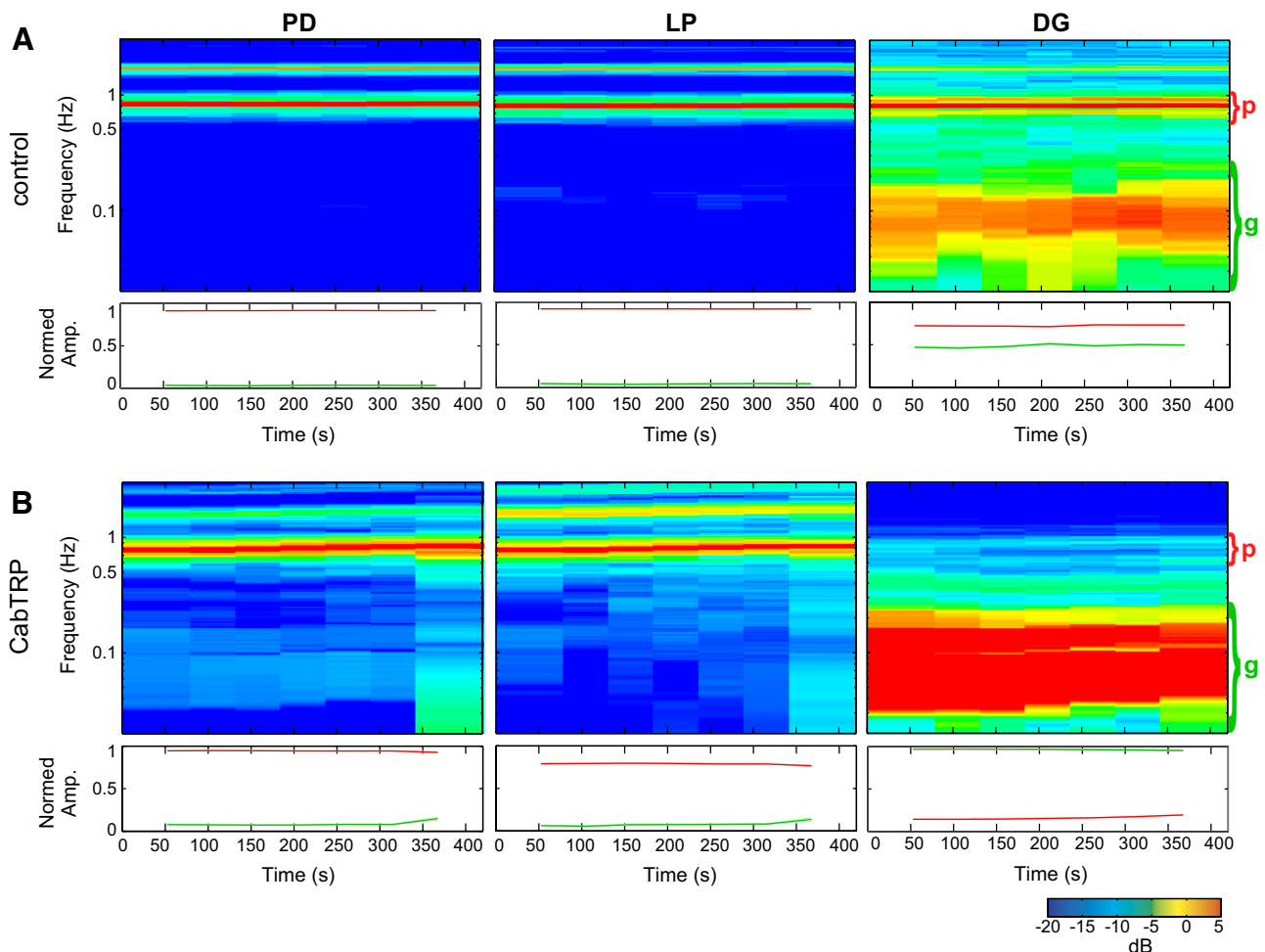


FIG. 12. Spectrograms of adult LP, PD, and DG activity in control saline and in CabTRP. Spectrograms of activity shown in Fig. 11. A: in control saline. B: in 10^{-6} M CabTRP. Normed amplitudes of activity at pyloric (red) and gastric mill (green) frequencies are shown in plots below each spectrogram.

amplitude = 0.69 ± 0.09 ; unpaired *t*-test, $P = 0.43$; adult, $n = 7$; embryo, $n = 13$).

We wanted to quantify the difference in frequency between the adult pyloric rhythm and the embryonic-fast activity. Using the peak frequency of lpm as a measure of the embryonic-fast frequency (see METHODS), we found that the mean embryonic-fast frequency (0.50 ± 0.21 Hz, $n = 25$) was significantly slower than the mean adult pyloric frequency (0.81 ± 0.10 , $n = 14$; unpaired *t*-test, $P < 0.0001$). This is consistent with previous reports, which established that the embryonic-fast activity was slower than the adult pyloric rhythm (Richards et al. 1999).

We were curious to know how the phase relationships of the embryonic-fast activity compared with those of the adult pyloric rhythm. The phase relationships of the embryonic-fast activity and the adult pyloric rhythm, as assessed by the peak coherence, are shown in Fig. 10. In both embryos and adults, PD activity alternated with LP (Fig. 10, *A* and *B*). In all of the embryonic gastric mill neurons, the activity occurred in the later part of the lpm cycle, but activity in both lgm and mgm was closer to firing synchronously with lpm, and dgm activity was closer to alternating with lpm (Fig. 10*A*). Pyloric-timed activity in adult DG and LG were significantly earlier in the LP cycle than in the embryonic-fast rhythm (statistics in figure legend). Thus PD and MG phasing was similar in the adult pyloric rhythm and the embryonic-fast activity, but LG and DG phasing was different.

We were unable to meaningfully compare the frequency of the slow activity in embryonic (<0.19 Hz; range, 0.1–0.3 Hz) and adult (<0.3 Hz; range, 0.1–0.3 Hz) gastric mill neurons; in 5/10 dgm, 5/10 mgm, and all of the 5 lgm embryonic recordings, there was no well-defined band of embryonic-slow activity with a clear upper and lower limit in frequency. Instead, the embryonic-slow activity was diffuse and spread over a broad range of frequencies. However, in dual recordings from gastric mill neurons in the same embryonic preparation, slow activity occurred at a similar frequency in four of five dgm/mgm recordings (data not shown). The peak coherence phase of this slow activity did not appear to be identical in embryos and adults (embryos at ~ 0 , adults at ~ 0.25).

CabTRP effects on adult motor patterns

We have shown that embryonic dgm and mgm display significant embryonic-slow activity. Although this activity is likely a precursor to the adult gastric mill rhythm (see DISCUSSION), it is weaker and more irregular than the adult gastric mill rhythm. Why might this be? One possible explanation is that, in the adult, certain neuromodulators are supplied by descending inputs to the STG, and these modulators are diminished or absent in the embryo. Previous studies in the adult STG have shown that neuromodulators can alter the extent to which neurons participate in the pyloric or gastric mill motor patterns (Marder and Bucher 2007). One modulator, CabTRP, can increase slow activity in gastric mill neurons of the crab, *C. borealis*. Furthermore, CabTRP is absent from the descending inputs in the embryonic STG but is present in the adult (Cape et al. 2008; Fénelon et al. 1999). Therefore the relative weakness of the slow activity in embryonic gastric mill neurons could be explained by the absence of CabTRP from the embryonic inputs (Cape et al. 2008; Fénelon et al. 1999).

We first examined the effects of CabTRP on the gastropyloric motor patterns of the adult lobster. CabTRP did not have obvious effects on LP and PD neurons, but it eliminated pyloric-timed activity in DG, allowing the gastric mill rhythm to predominate (Fig. 11, *A* and *B*). Figure 12 shows the spectrograms of the traces in Fig. 11. In control conditions and in CabTRP, most of the activity in LP and PD occurred around 0.8 Hz (Fig. 12, *A* and *B*). In control, the DG neuron showed two very different frequencies in its activity: a pyloric-timed activity (~ 0.8 Hz) and a gastric-timed activity (<0.2 Hz; Fig. 12*A*, right). In CabTRP, the pyloric activity disappeared, and most of the DG activity occurred at the gastric mill frequency (Fig. 12*B*, right).

CabTRP makes embryonic motor patterns more adult-like

In the embryo, CabTRP increased the amount of embryonic-slow activity in dgm, thus transforming the embryonic motor pattern into a more adult-like form. Figure 13 shows simultaneous intracellular recordings of activity in lpm, pdm, and dgm in one embryo preparation. In control saline, the frequency of lpm, pdm, and dgm activity was 0.3 Hz (Fig. 13*A*). When CabTRP was bath applied, the frequency of lpm and pdm activity increased to 0.42 Hz, but the most prominent effect of CabTRP was on dgm, in which CabTRP produced intermittent pauses (Fig. 13*B*).

This effect can also be seen in the spectrograms calculated from the traces shown in Fig. 13 (Fig. 14). The pdm spectrograms are grossly similar between control and CabTRP treatments, as are the lpm spectrograms (Fig. 14, *A* and *B*). The dgm spectrograms, in contrast, show a pronounced low-frequency band in the CabTRP condition, reflecting the intermittent pauses in the dgm activity observed in CabTRP (Fig. 14*B*).

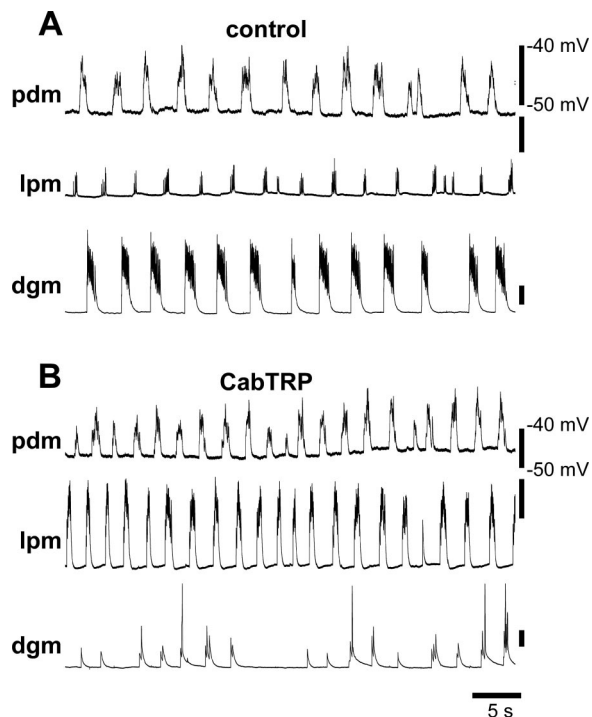


FIG. 13. Embryonic lpm, pdm, and dgm activity in control saline and in CabTRP. Simultaneous intracellular recordings from embryonic lpm, pdm, and dgm. *A*: in control saline. *B*: in 10^{-6} M CabTRP.

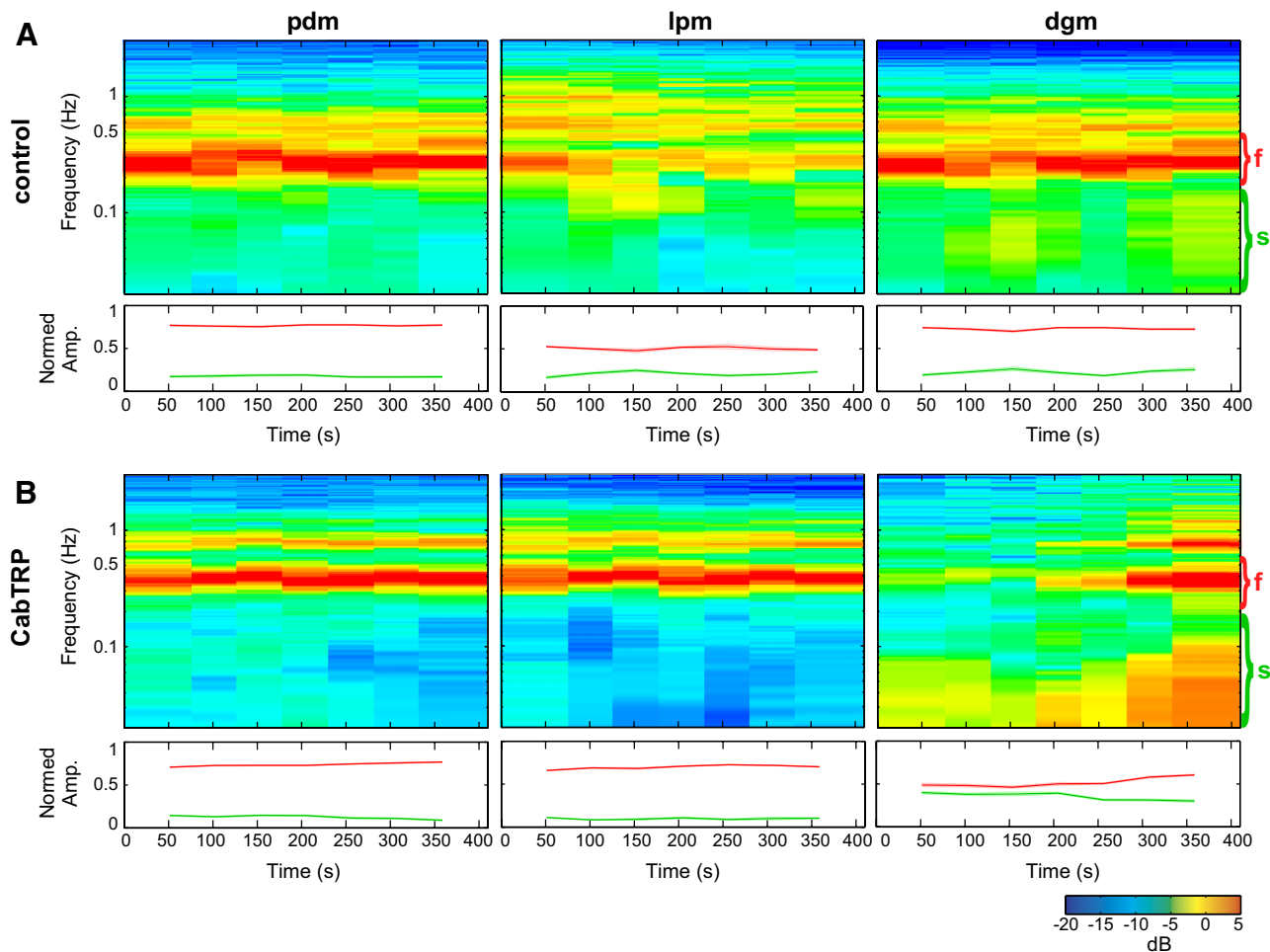


FIG. 14. Spectrograms of embryonic lpm, pdm, and dgm activity in control saline and in CabTRP. Spectrograms of activity shown in Fig. 13. *A*: in control saline. *B*: in 10^{-6} M CabTRP. Normed amplitudes of activity at embryonic-fast (red) and embryonic-slow (green) frequencies are shown in plots below each spectrogram.

Summary of embryonic and adult motor patterns in CabTRP

The effects of CabTRP on the amount of slow and fast activity were similar, although not identical, in embryos and adults (Fig. 15). CabTRP significantly increased the amount of slow activity in both adult DG and embryonic dgm (Fig. 15, *A–D*; statistics in figure legend). CabTRP also significantly increased the amount of slow activity in adult LP and PD neurons and decreased the amount of fast activity in adult LP and DG neurons (Fig. 15, *A* and *B*; statistics in figure legend).

CabTRP had different effects on the pyloric rhythm in the adult and the embryonic-fast activity in the embryo. CabTRP increased the mean frequency of the embryonic-fast rhythm from 0.38 ± 0.08 to 0.52 ± 0.06 Hz (frequency of pdm activity, $n = 7$; paired *t*-test, $P < 0.01$). In the adult, CabTRP did not significantly increase the pyloric frequency [frequency of PD activity = 0.82 ± 0.06 Hz (control), 0.88 ± 0.06 Hz (CabTRP); paired *t*-test, $P = 0.12$; $n = 7$]. CabTRP did not have a significant effect on the peak coherence phase of the fast activity in LP and DG relative to PD in the embryo or the adult (circular analog of paired *t*-test; see METHODS; adult LP, $P = 0.61$; embryo lpm, $P = 0.19$; adult DG, $P = 0.19$; embryo dgm, $P = 0.29$).

DISCUSSION

It is widely known that many developing neuronal networks are rhythmically active before they are used, but this early activity is usually different from that in the adult. We used long simultaneous recordings and spectral analysis to show that before eating, the late embryonic stomatogastric nervous system can reliably produce activity that presages adult activity.

Spectrograms to measure fast and slow activity

To quantify the amount of fast and slow activity in the embryonic recordings, we calculated spectrograms, a method commonly used for acoustical, thermal, seismic, and electromagnetic signals (Thomson 2000). Biologists have used spectrograms to analyze a wide variety of phenomena, including acoustic communication (e.g., birdsong) (Margoliash 1997; Marler 1969), behavioral and circadian oscillations (Dolezelova et al. 2007; Dowse 2007; Levine et al. 2002; Sanyal et al. 2006), and rhythmic activity in neuronal networks (Bucher et al. 2006; Miller and Sigvardt 1998; Richards et al. 1999). These tools, although not commonly used for analyses of central pattern generating networks, will be invaluable for the study of motor patterns and other rhythms, especially in genetically tractable

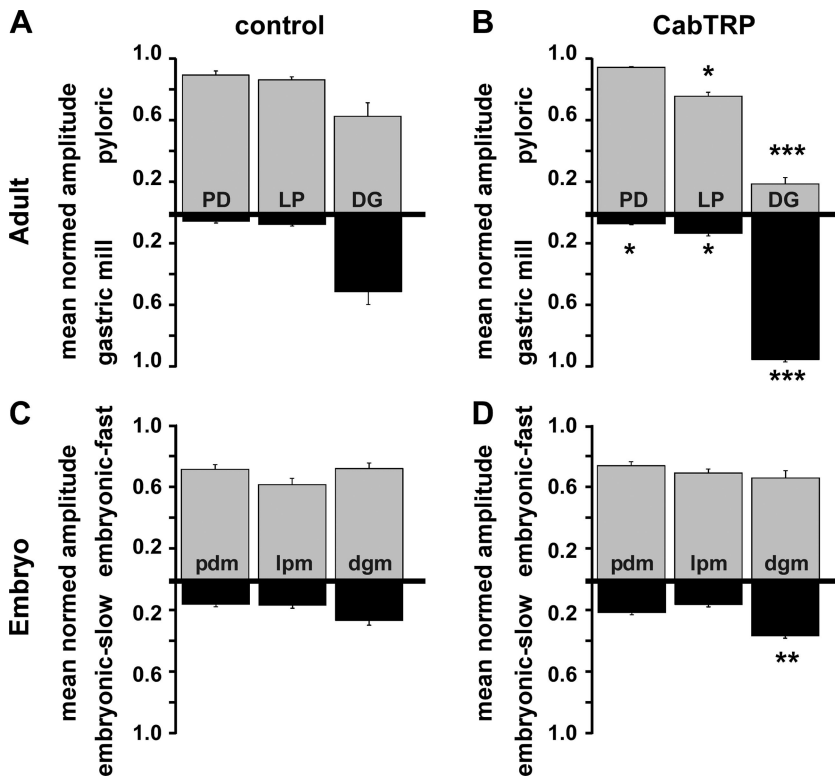


FIG. 15. Summary of CabTRP effects on embryonic-fast, embryonic-slow, adult pyloric, and adult gastric mill activity. *A*: mean normed amplitudes of pyloric (gray) and gastric mill (black) activity in adult PD, LP, and DG in control saline. *B*: the same quantities in 10^{-6} M CabTRP. For all adult neurons, the normed gastric amplitude was significantly higher in CabTRP compared with control saline (paired *t*-test: LP, $P = 0.03$, $n = 7$; PD, $P = 0.04$, $n = 7$; DG, $P = 0.0008$, $n = 7$). Normed pyloric amplitudes were significantly lower in CabTRP compared with control saline for adult LP (paired *t*-test, $P = 0.013$, $n = 7$) and DG (paired *t*-test, $P = 0.0008$, $n = 7$). *C*: mean normed amplitudes of embryonic-fast and embryonic-slow activity in embryonic pdm, lpm, and dgm in control saline. *D*: the same quantities in 10^{-6} M CabTRP. The normed slow amplitude of activity in embryonic dgm was significantly lower in CabTRP compared with control saline (paired *t*-test, $P = 0.008$, $n = 7$). In all panels, a significant difference from control conditions is indicated by asterisks: * $P < 0.05$, ** $P < 0.01$, *** $P < 0.001$.

model organisms. In such animals, genetic manipulations commonly generate erratic and irregular neuronal and behavioral phenotypes, which nonetheless must still be assayed for rhythmicity (Dixit et al. 2008; Dolezelova et al. 2007; Ebert et al. 2005; Fox et al. 2006; Kopp et al. 2005; Nitabach et al. 2006; Sanyal et al. 2006).

We used spectrograms because traditional methods of analysis require unambiguous burst detection, which was not possible for many embryonic recordings, and because spectral analysis was used in a previous study to quantify the relative amount of slow and fast activity in the adult lobster STNS (Bucher et al. 2006). In this study, we analyzed relatively long stretches of data (10–110 min). These long recordings enabled us to show for the first time that embryonic gastric mill neurons produced significantly more embryonic-slow activity than pyloric neurons and that the frequency of both the fast and slow activity varied across the recordings. This lack of stationarity could be caused by changes in activity in descending modulatory inputs, a result of sensory feedback, or result from networks that are less tightly tuned in the adult, and that may be intrinsically “noisy” in their output. This kind of intermittent output is reminiscent of the “bouting” seen in preparations of the crab STG that recover rhythmicity after the removal of modulatory inputs (Khorkova and Golowasch 2007; Luther et al. 2003), presumably as the network retunes itself.

Coherograms to estimate phase

The phase relationships of activity in stomatogastric neurons are typically defined as the relative onset and offset of each burst (Selverston and Moulins 1987). Although both we and Le Feuvre et al. (1999) recorded short sequences of data in which conventional burst analyses was feasible, the

lack of stationarity in long recordings in which irregular sequences were interspersed with more regular stretches precluded its use in all but selected short stretches of data. In contrast to burst detection methods, coherograms allowed us to calculate the stability of the phase relationships over extended time periods. The coherogram-derived phase relationships of embryonic-fast activity were stable and similar to those determined by burst onset/offset (Le Feuvre et al. 1999), but the phase relationships of the slow activity were quite variable. When comparing adults and embryos, we found that phase relationships of the output from embryonic and adult PD/LP and MG/LP neurons were not statistically different, and LG/LP and DG/LP phases were different across development.

Comparison of embryonic and adult activity

We suggest that the embryonic-fast activity in pyloric neurons is an immature form of the adult pyloric rhythm because 1) the output from embryonic LP and PD neurons fire out of phase, as they do in the adult, and 2) during larval development, embryonic-fast activity from LP neurons becomes faster and more regular, becoming more adult-like by the end of larval stage (Richards et al. 1999). Fast activity was also produced by embryonic gastric mill neurons, as it is by adult gastric mill neurons, particularly DG neurons when the gastric mill rhythm is present (Bucher et al. 2006). However, the relative phase of this fast activity in LG and DG neurons was different in embryos and adults. Modeling work (Bem et al. 2002) suggests that electrical coupling, which is believed to be higher in embryonic STG (Ducret et al. 2006, 2007), could be responsible for a greater degree of synchrony, perhaps contributing to the developmental differences of the LG and DG phase relationships.

It is tempting to propose that the embryonic-slow activity is an immature form of the adult gastric mill rhythm. Evidence in favor of this hypothesis is the observation that embryonic-slow activity was reliably present only in gastric mill neurons. Furthermore, in a small set of experiments, the frequency of the embryonic-slow activity was similar in all monitored gastric mill neurons from the same embryonic preparation. On the other hand, the phase of this slow activity was not identical in embryos and adults. However, the phase of the gastric mill neurons can vary considerably depending on how the gastric mill rhythms are elicited (Blitz et al. 1999; Combes et al. 1999a,b; Heinzel and Selverston 1988; Norris et al. 1994). Therefore it is difficult to know whether the differences in phase are indications of different forms of "gastric-like" activity or caused by a fundamental immaturity of the network.

Effects of CabTRP on adult STNS motor patterns

In the adult STG, neurons can simultaneously exhibit both fast and slow rhythmic activity, to varying degrees (Bucher et al. 2006; Weimann and Marder 1994; Weimann et al. 1991). Sensory and neuromodulatory input can influence the amount of fast and slow activity by altering neuronal excitability and/or synaptic strengths (Hooper and Moulins 1989; Weimann et al. 1990, 1993). In the gastric mill neurons of the crab *C. borealis*, CabTRP enhances slow activity, presumably by increasing the excitability of the gastric neurons, changing synaptic strengths between the gastric neurons, or decreasing the synaptic strengths from pyloric neurons onto gastric mill neurons (Wood et al. 2000). In the adult lobster, CabTRP strongly enhanced gastric bursting. In fact, the decreased pyloric-timed activity seen in the DG neuron (Fig. 11) might indicate that CabTRP is down-regulating the synaptic interactions from pyloric neurons onto gastric mill neurons.

Effects of CabTRP on embryonic STNS motor patterns

During development, CabTRP appears in the neuromodulatory inputs at the end of larval development (Cape et al. 2008; Fénelon et al. 1999). Therefore the absence of CabTRP in the embryonic inputs could help explain why embryonic motor patterns are immature. Consistent with this, we found that CabTRP significantly increased the amount of slow activity produced by embryonic gastric mill neurons, producing a motor pattern that looked more like adult motor patterns. Perhaps as CabTRP arrives in the late larval STG, it increases the ability of gastric neurons to generate long bursts by acting on the intrinsic excitability of DG neurons and/or the synaptic strengths between gastric mill and pyloric neurons, as suggested by the CabTRP effects in the adult (Wood et al. 2000).

The finding that CabTRP had similar effects on embryonic and adult stomatogastric motor patterns supports previous results suggesting that the embryonic STG network is mature by the end of embryonic development (Le Feuvre et al. 1999) and that the immaturity of embryonic motor patterns is best explained by the immaturity of the neuromodulatory inputs (Ducret et al. 2007; Fénelon et al. 1999; Kilman et al. 1999). However, adult and embryonic motor patterns were not identical in CabTRP. These results could be explained by a greater

degree of electrical coupling in the embryonic STG (Bem et al. 2002; Ducret et al. 2006, 2007), a difference in the intrinsic excitability of the neurons, or a difference in the expression of CabTRP receptors.

Role of sensory feedback in embryonic and adult STNS motor patterns

In the embryonic experiments, we used the whole stomach, with sensory neurons left attached, whereas for the adult experiments we used the isolated STNS, which lacks many sensory neurons. Therefore it is possible that the presence of sensory feedback in the embryonic preparations could partially account for the differences between embryos and adults. In the STNS, a number of sensory pathways are important for activating gastric mill rhythms (Beenhakker and Nusbaum 2004; Beenhakker et al. 2004, 2005, 2007; Blitz et al. 2004; Christie et al. 2004). In the adult, dissected intact STNS, the descending modulatory neurons ordinarily activated by sensory neurons may be constitutively active, accounting for ongoing gastric mill rhythms. However, in juvenile adult preparations, gastric mill and pyloric rhythms were similar in the isolated STNS and in whole stomachs with all sensory feedback pathways intact (data not shown), suggesting that the difference in sensory input may play a relatively minor role in the effects described here.

It is not clear what role sensory input plays in regulating embryonic STNS rhythms. At least one key set of stretch receptors, the gastropyloric stretch receptor (GPR) neurons, do not contain the full adult complement of neuromodulators in the embryo (Fénelon et al. 1999; Kilman et al. 1999; Richards et al. 2003). This immaturity could reduce the influence of embryonic sensory input, especially if the neuromodulators that activate the descending pathways are those that are missing until later in development or if the descending pathways activated by those sensory neurons release modulators that are absent in the embryo.

Conclusions

It has been suggested in numerous studies that rhythmic activity during development is needed for proper construction and tuning of adult circuits (Gonzalez-Islas and Wenner 2006; Katz and Shatz 1996), and changes in this activity are thought to influence specific developmental events (Gu and Spitzer 1995; Hanson and Landmesser 2004, 2006). The synapses between the STG neurons and their final muscle targets are well established quite early in development, and the embryonic rhythmic STG activity could be serving not only to tune the STG networks themselves, but also to ensure that the appropriate neuromuscular connections are established and maintained (Pulver et al. 2005). It is an open question of whether the slower activity seen here is important for tuning the properties of the gastric mill neurons or whether the faster activity is sufficient to play this role. It is tempting to speculate that some features of an adult gastric mill neuron functional identity may require that they express some slow dynamics early in life.

ACKNOWLEDGMENTS

We thank Dr. Dirk M. Bucher (The Whitney Laboratory for Marine Bioscience) for participation in the development of the spectral analysis

methods, for the use of some of his data in Fig. 10, and in the comparison of adult and embryonic motor patterns in control conditions. We also thank Dr. Michael P. Nusbaum at the University of Pennsylvania for the gift of the CabTRP peptide.

GRANTS

This work was supported by National Institute of Neurological Disorders and Stroke Grants NS-050479 to K. J. Rehm, NS-017813 to E. Marder, and NS-050928 to A. L. Taylor.

REFERENCES

- Beenhakker MP, Blitz DM, Nusbaum MP.** Long-lasting activation of rhythmic neuronal activity by a novel mechanosensory system in the crustacean stomatogastric nervous system. *J Neurophysiol* 91: 78–91, 2004.
- Beenhakker MP, DeLong ND, Saideman SR, Nadim F, Nusbaum MP.** Proprioceptor regulation of motor circuit activity by presynaptic inhibition of a modulatory projection neuron. *J Neurosci* 25: 8794–8806, 2005.
- Beenhakker MP, Kirby MS, Nusbaum MP.** Mechanosensory gating of proprioceptor input to modulatory projection neurons. *J Neurosci* 27: 14308–14316, 2007.
- Beenhakker MP, Nusbaum MP.** Mechanosensory activation of a motor circuit by coactivation of two projection neurons. *J Neurosci* 24: 6741–6750, 2004.
- Bekoff A.** Ontogeny of leg motor output in the chick embryo: a neural analysis. *Brain Res* 106: 271–291, 1976.
- Bem T, Le Feuvre Y, Simmers J, Meyrand P.** Electrical coupling can prevent expression of adult-like properties in an embryonic neural circuit. *J Neurophysiol* 87: 538–547, 2002.
- Ben-Ari Y.** Developing networks play a similar melody. *Trends Neurosci* 24: 353–360, 2001.
- Blitz DM, Beenhakker MP, Nusbaum MP.** Different sensory systems share projection neurons but elicit distinct motor patterns. *J Neurosci* 24: 11381–11390, 2004.
- Blitz DM, Christie AE, Coleman MJ, Norris BJ, Marder E, Nusbaum MP.** Different proctolin neurons elicit distinct motor patterns from a multifunctional neuronal network. *J Neurosci* 19: 5449–5463, 1999.
- Blitz DM, Christie AE, Marder E, Nusbaum MP.** Distribution and effects of tachykinin-like peptides in the stomatogastric nervous system of the crab, *Cancer borealis*. *J Comp Neurol* 354: 282–294, 1995.
- Bucher D, Prinz AA, Marder E.** Animal-to-animal variability in motor pattern production in adults and during growth. *J Neurosci* 25: 1611–1619, 2005.
- Bucher D, Taylor AL, Marder E.** Central pattern generating neurons simultaneously express fast and slow rhythmic activities in the stomatogastric ganglion. *J Neurophysiol* 95: 3617–3632, 2006.
- Cang J, Renteria RC, Kaneko M, Liu X, Copenhagen DR, Stryker MP.** Development of precise maps in visual cortex requires patterned spontaneous activity in the retina. *Neuron* 48: 797–809, 2005.
- Cape SS, Rehm KJ, Ma M, Marder E, Li L.** Mass spectral comparison of the neuropeptide complement of the stomatogastric ganglion and brain in the adult and embryonic lobster, *Homarus americanus*. *J Neurochem* 105: 690–708, 2008.
- Casasnovas B, Meyrand P.** Functional differentiation of adult neural circuits from a single embryonic network. *J Neurosci* 15: 5703–5718, 1995.
- Christie AE, Lundquist CT, Nässel DR, Nusbaum MP.** Two novel tachykinin-related peptides from the nervous system of the crab, *Cancer borealis*. *J Exp Biol* 200: 2279–2294, 1997.
- Christie AE, Stein W, Quinlan JE, Beenhakker MP, Marder E, Nusbaum MP.** Actions of a histaminergic/peptidergic projection neuron on rhythmic motor patterns in the stomatogastric nervous system of the crab, *Cancer borealis*. *J Comp Neurol* 469: 153–169, 2004.
- Combes D, Merrywest SD, Simmers J, Sillar KT.** Developmental segregation of spinal networks driving axial- and hindlimb-based locomotion in metamorphosing *Xenopus laevis*. *J Physiol* 559: 17–24, 2004.
- Combes D, Meyrand P, Simmers J.** Dynamic restructuring of a rhythmic motor program by a single mechanoreceptor neuron in lobster. *J Neurosci* 19: 3620–3628, 1999a.
- Combes D, Meyrand P, Simmers J.** Motor pattern specification by dual descending pathways to a lobster rhythm-generating network. *J Neurosci* 19: 3610–3619, 1999b.
- Demas J, Eglén SJ, Wong RO.** Developmental loss of synchronous spontaneous activity in the mouse retina is independent of visual experience. *J Neurosci* 23: 2851–2860, 2003.
- Demas J, Sagdullaev BT, Green E, Jaubert-Miazza L, McCall MA, Gregg RG, Wong RO, Guido W.** Failure to maintain eye-specific segregation in nob, a mutant with abnormally patterned retinal activity. *Neuron* 50: 247–259, 2006.
- Dixit R, Vijayraghavan K, Bate M.** Hox genes and the regulation of movement in *Drosophila*. *Dev Neurobiol* 68: 309–316, 2008.
- Dolezelova E, Dolezel D, Hall JC.** Rhythm defects caused by newly engineered null mutations in *Drosophila*'s cryptochrome gene. *Genetics* 177: 329–345, 2007.
- Dowse HB.** Statistical analysis of biological rhythm data. In: *Circadian Rhythms: Methods and Protocols*, edited by Rosato E. Totowa, NJ: Humana Press, 2007, p. 29–45.
- Ducret E, Alexopoulos H, Le Feuvre Y, Davies JA, Meyrand P, Bacon JP, Fénelon VS.** Innexins in the lobster stomatogastric nervous system: cloning, phylogenetic analysis, developmental changes and expression within adult identified dye and electrically coupled neurons. *Eur J Neurosci* 24: 3119–3133, 2006.
- Ducret E, Le Feuvre Y, Meyrand P, Fénelon VS.** Removal of GABA within adult modulatory systems alters electrical coupling and allows expression of an embryonic-like network. *J Neurosci* 27: 3626–3638, 2007.
- Ebert AM, Hume GL, Warren KS, Cook NP, Burns CG, Mohideen MA, Siegal G, Yelon D, Fishman MC, Garrity DM.** Calcium extrusion is critical for cardiac morphogenesis and rhythm in embryonic zebrafish hearts. *Proc Natl Acad Sci USA* 102: 17705–17710, 2005.
- Fénelon VS, Kilman V, Meyrand P, Marder E.** Sequential developmental acquisition of neuromodulatory inputs to a central pattern-generating network. *J Comp Neurol* 408: 335–351, 1999.
- Fischer KF, Lukasiewicz PD, Wong RO.** Age-dependent and cell class-specific modulation of retinal ganglion cell bursting activity by GABA. *J Neurosci* 18: 3767–3778, 1998.
- Fox LE, Soll DR, Wu CF.** Coordination and modulation of locomotion pattern generators in *Drosophila* larvae: effects of altered biogenic amine levels by the tyramine beta hydroxylase mutation. *J Neurosci* 26: 1486–1498, 2006.
- Garaschuk O, Hanse E, Konnerth A.** Developmental profile and synaptic origin of early network oscillations in the CA1 region of rat neonatal hippocampus. *J Physiol* 507: 219–236, 1998.
- Goldberg D, Nusbaum MP, Marder E.** Substance P-like immunoreactivity in the stomatogastric nervous systems of the crab *Cancer borealis* and the lobsters *Panulirus interruptus* and *Homarus americanus*. *Cell Tissue Res* 252: 515–522, 1988.
- Gonzalez-Islas C, Wenner P.** Spontaneous network activity in the embryonic spinal cord regulates AMPAergic and GABAergic synaptic strength. *Neuron* 49: 563–575, 2006.
- Greer JJ, Funk GD, Ballanyi K.** Preparing for the first breath: prenatal maturation of respiratory neural control. *J Physiol* 570: 437–444, 2006.
- Gu X, Spitzer NC.** Distinct aspects of neuronal differentiation encoded by frequency of spontaneous Ca^{2+} transients. *Nature* 375: 784–787, 1995.
- Hanson MG, Landmesser LT.** Characterization of the circuits that generate spontaneous episodes of activity in the early embryonic mouse spinal cord. *J Neurosci* 23: 587–600, 2003.
- Hanson MG, Landmesser LT.** Normal patterns of spontaneous activity are required for correct motor axon guidance and the expression of specific guidance molecules. *Neuron* 43: 687–701, 2004.
- Hanson MG, Landmesser LT.** Increasing the frequency of spontaneous rhythmic activity disrupts pool-specific axon fasciculation and pathfinding of embryonic spinal motoneurons. *J Neurosci* 26: 12769–12780, 2006.
- Harris-Warrick RM, Marder E, Selverston AI, Moulins M.** *Dynamic Biological Networks. The Stomatogastric Nervous System*. Cambridge, MA: MIT Press, 1992.
- Heinzel HG.** Gastric mill activity in the lobster. I. Spontaneous modes of chewing. *J Neurophysiol* 59: 528–550, 1988.
- Heinzel HG, Selverston AI.** Gastric mill activity in the lobster. III. Effects of proctolin on the isolated central pattern generator. *J Neurophysiol* 59: 566–585, 1988.
- Helluy SM, Beltz BS.** Embryonic development of the american lobster (*Homarus americanus*) - quantitative staging and characterization of an embryonic molt cycle. *Biol Bull* 180: 355–371, 1991.
- Hooks BM, Chen C.** Distinct roles for spontaneous and visual activity in remodeling of the retinogeniculate synapse. *Neuron* 52: 281–291, 2006.
- Hooper SL, Moulins M.** Switching of a neuron from one network to another by sensory-induced changes in membrane properties. *Science* 244: 1587–1589, 1989.

- Huberman AD, Speer CM, Chapman B.** Spontaneous retinal activity mediates development of ocular dominance columns and binocular receptive fields in v1. *Neuron* 52: 247–254, 2006.
- Jarvis MR, Mitra PP.** Sampling properties of the spectrum and coherency of sequences of action potentials. *Neural Comput* 13: 717–749, 2001.
- Katz LC, Shatz CJ.** Synaptic activity and the construction of cortical circuits. *Science* 274: 1133–1138, 1996.
- Khorkova O, Golowasch J.** Neuromodulators, not activity, control coordinated expression of ionic currents. *J Neurosci* 27: 8709–8718, 2007.
- Kilman V, Fénelon VS, Richards KS, Thirumalai V, Meyrand P, Marder E.** Sequential developmental acquisition of cotransmitters in identified sensory neurons of the stomatogastric nervous system of the lobsters, *Homarus americanus* and *Homarus gammarus*. *J Comp Neurol* 408: 318–334, 1999.
- Kopp R, Schwerte T, Pelster B.** Cardiac performance in the zebrafish breakdance mutant. *J Exp Biol* 208: 2123–2134, 2005.
- Le Feuvre Y, Fénelon VS, Meyrand P.** Central inputs mask multiple adult neural networks within a single embryonic network. *Nature* 402: 660–664, 1999.
- Leinekugel X, Khazipov R, Cannon R, Hirase H, Ben-Ari Y, Buzsaki G.** Correlated bursts of activity in the neonatal hippocampus *in vivo*. *Science* 296: 2049–2052, 2002.
- Levine JD, Funes P, Dowse HB, Hall JC.** Signal analysis of behavioral and molecular cycles. *BMC Neurosci* 3: 1, 2002.
- Luther JA, Robie AA, Yarotsky J, Reina C, Marder E, Golowasch J.** Episodic bouts of activity accompany recovery of rhythmic output by a neuromodulator- and activity-deprived adult neural network. *J Neurophysiol* 90: 2720–2730, 2003.
- Marder E, Bucher D.** Understanding circuit dynamics using the stomatogastric nervous system of lobsters and crabs. *Annu Rev Physiol* 69: 291–316, 2007.
- Mardia KV, Jupp PE.** *Directional Statistics*. Baffins Lane, UK: Wiley, 1999, p. 122.
- Margoliash D.** Distributed time-domain representations in the birdsong system. *Neuron* 19: 963–966, 1997.
- Marler P.** Tonal quality of bird sounds. In: *Bird Vocalizations*, edited by Hinde RA. London: Cambridge, 1969, p. 5–27.
- Mehta V, Sernagor E.** Early neural activity and dendritic growth in turtle retinal ganglion cells. *Eur J Neurosci* 24: 773–786, 2006.
- Miller WL, Sigvardt KA.** Spectral analysis of oscillatory neural circuits. *J Neurosci Methods* 80: 113–128, 1998.
- Milner LD, Landmesser LT.** Cholinergic and GABAergic inputs drive patterned spontaneous motoneuron activity before target contact. *J Neurosci* 19: 3007–3022, 1999.
- Moody WJ, Bosma MM.** Ion channel development, spontaneous activity, and activity-dependent development in nerve and muscle cells. *Physiol Rev* 85: 883–941, 2005.
- Mulloney B.** Organization of the stomatogastric ganglion of the spiny lobster. V. Coordination of the gastric and pyloric systems. *J Comp Physiol* 122: 227–240, 1977.
- Nishimaru H, Kudo N.** Formation of the central pattern generator for locomotion in the rat and mouse. *Brain Res Bull* 53: 661–669, 2000.
- Nitabach MN, Wu Y, Sheeba V, Lemon WC, Strumbos J, Zelensky PK, White BH, Holmes TC.** Electrical hyperexcitation of lateral ventral pacemaker neurons desynchronizes downstream circadian oscillators in the fly circadian circuit and induces multiple behavioral periods. *J Neurosci* 26: 479–489, 2006.
- Norris BJ, Coleman MJ, Nusbaum MP.** Recruitment of a projection neuron determines gastric mill motor pattern selection in the stomatogastric nervous system of the crab, *Cancer borealis*. *J Neurophysiol* 72: 1451–1463, 1994.
- Nusbaum MP, Blütz DM, Swensen AM, Wood D, Marder E.** The roles of co-transmission in neural network modulation. *Trends Neurosci* 24: 146–154, 2001.
- O'Donovan MJ.** The origin of spontaneous activity in developing networks of the vertebrate nervous system. *Curr Opin Neurobiol* 9: 94–104, 1999.
- Pagliardini S, Ren J, Greer JJ.** Ontogeny of the pre-Bötzinger complex in perinatal rats. *J Neurosci* 23: 9575–9584, 2003.
- Penn AA, Riquelme PA, Feller MB, Shatz CJ.** Competition in retinogeniculate patterning driven by spontaneous activity. *Science* 279: 2108–2112, 1998.
- Percival DB, Walden AT.** *Spectral Analysis for Physical Applications: Multitaper and Conventional Univariate Techniques*. Cambridge, UK: Cambridge, 1993.
- Pulver SR, Bucher D, Simon DJ, Marder E.** Constant amplitude of postsynaptic responses for single presynaptic action potentials but not bursting input during growth of an identified neuromuscular junction in the lobster, *Homarus americanus*. *J Neurobiol* 62: 47–61, 2005.
- Ren J, Greer JJ.** Ontogeny of rhythmic motor patterns generated in the embryonic rat spinal cord. *J Neurophysiol* 89: 1187–1195, 2003.
- Richards KS.** *Development and Modulation of the Stomatogastric Motor Patterns of the Lobster, Homarus Americanus* (PhD thesis). Waltham, MA: Brandeis University, 2000.
- Richards KS, Miller WL, Marder E.** Maturation of lobster stomatogastric ganglion rhythmic activity. *J Neurophysiol* 82: 2006–2009, 1999.
- Richards KS, Simon DJ, Pulver SR, Beltz BS, Marder E.** Serotonin in the developing stomatogastric system of the lobster, *Homarus americanus*. *J Neurobiol* 54: 380–392, 2003.
- Sanyal S, Jennings T, Dowse H, Ramaswami M.** Conditional mutations in SERCA, the Sarco-endoplasmic reticulum Ca²⁺-ATPase, alter heart rate and rhythmicity in *Drosophila*. *J Comp Physiol [B]* 176: 253–263, 2006.
- Selverston AI, Moulins M.** *The Crustacean Stomatogastric System*. Berlin, Germany: Springer-Verlag, 1987.
- Sernagor E, Eglén SJ, Wong RO.** Development of retinal ganglion cell structure and function. *Prog Retinal Eye Res* 20: 139–174, 2001.
- Sharp AA, Ma E, Bekoff A.** Developmental changes in leg coordination of the chick at embryonic days 9, 11, and 13: uncoupling of ankle movements. *J Neurophysiol* 82: 2406–2414, 1999.
- Stellwagen D, Shatz CJ.** An instructive role for retinal waves in the development of retinogeniculate connectivity. *Neuron* 33: 357–367, 2002.
- Thirumalai V, Marder E.** Colocalized neuropeptides activate a central pattern generator by acting on different circuit targets. *J Neurosci* 22: 1874–1882, 2002.
- Thomson DJ.** Multitaper analysis of nonstationary and nonlinear time series data. In: *Nonlinear and Nonstationary Signal Processing*, edited by Fitzgerald WJ, Smith RL, Walden AT, Young PC. Cambridge, UK: Cambridge, 2000, p. 317–394.
- Thomson DJ, Chave AD.** Jackknifed error estimates for spectra, coherences, and transfer functions. In: *Advances in Spectrum Analysis and Array Processing*, edited by Haykin S. Englewood Cliffs, NJ: Prentice-Hall, 1991.
- Thuma JB, Hooper SL.** Quantification of gastric mill network effects on a movement related parameter of pyloric network output in the lobster. *J Neurophysiol* 87: 2372–2384, 2002.
- Torborg CL, Feller MB.** Spontaneous patterned retinal activity and the refinement of retinal projections. *Prog Neurobiol* 76: 213–235, 2005.
- Upton GJG.** Single-sample tests for the von Mises distribution. *Biometrika* 60: 87–99, 1973.
- Warland DK, Huberman AD, Chalupa LM.** Dynamics of spontaneous activity in the fetal macaque retina during development of retinogeniculate pathways. *J Neurosci* 26: 5190–5197, 2006.
- Weimann JM, Marder E.** Switching neurons are integral members of multiple oscillatory networks. *Curr Biol* 4: 896–902, 1994.
- Weimann JM, Marder E, Evans B, Calabrese RL.** The effects of SDRN-FLRFamide and TNRNFLRFamide on the motor patterns of the stomatogastric ganglion of the crab, *Cancer borealis*. *J Exp Biol* 181: 1–26, 1993.
- Weimann JM, Meyrand P, Marder E.** Neurons that participate in several behaviors. In: *Frontiers in Crustacean Neurobiology*. Basel: Birkhauser Verlag, 1990, p. 424–430.
- Weimann JM, Meyrand P, Marder E.** Neurons that form multiple pattern generators: identification and multiple activity patterns of gastric/pyloric neurons in the crab stomatogastric system. *J Neurophysiol* 65: 111–122, 1991.
- Wong RO, Meister M, Shatz CJ.** Transient period of correlated bursting activity during development of the mammalian retina. *Neuron* 11: 923–938, 1993.
- Wong RO, Oakley DM.** Changing patterns of spontaneous bursting activity of on and off retinal ganglion cells during development. *Neuron* 16: 1087–1095, 1996.
- Wood DE, Stein W, Nusbaum MP.** Projection neurons with shared cotransmitters elicit different motor patterns from the same neural circuit. *J Neurosci* 20: 8943–8953, 2000.
- Yvert B, Branchereau P, Meyrand P.** Multiple spontaneous rhythmic activity patterns generated by the embryonic mouse spinal cord occur within a specific developmental time window. *J Neurophysiol* 91: 2101–2109, 2004.